# EXPERIMENTAL ANALYSIS AND MODELING OF SHEAR STRENGTH OF ADHESIVE-BONDED SINGLE-LAP GLASS FIBER REINFORCED COMPOSITES

**A Thesis Submitted to**
**the Graduate School of Engineering and Sciences of**
**İzmir Institute of Technology**
**in Partial Fulfilment of the Requirements for the Degree of**

**MASTER OF SCIENCE**

**in Mechanical Engineering**

**by**
**Sertaç SERBEST**

**March 2024**
**İZMİR**

We approve the thesis of **Sertaç SERBEST**

**Examining Committee Members:**

_____

**Prof. Dr. H. Seçil ARTEM**

Department of Mechanical Engineering, İzmir Institute of Technology

_____

**Assist. Prof. Dr. Fatih Toksoy**

Department of Mechanical Engineering, İzmir Institute of Technology

_____

**Assist. Prof. Dr. Ebubekir ATAN**

Department of Mechanical Engineering, İzmir Katip Çelebi University

**08 March 2024**

_____

**Prof. Dr. H. Seçil ARTEM**

Supervisor, Department of Mechanical Engineering,

İzmir Institute of Technology

_____

**Prof. Dr. M. İ. Can DEDE**

Head of the Department of Mechanical Engineering

_____

**Prof. Dr. Mehtap Eanes**

Dean of the Graduate School

# ACKNOWLEDGMENTS

I would like to thank my thesis advisor, Prof. Dr. H. Seçil ARTEM for her devoted support, guidance and encouraging approach during the learning and writing process of my master's thesis.

I would like to thank my mother Sevgül SERBEST, my father Cevat SERBEST and my brother Serhat SERBEST, who have always been by my side throughout my life, always supported the decisions I made, and always gave me courage and morale not only during this work process. I dedicate this thesis to my family.

I would like to thank my dear wife Buse Gül DOĞANAY SERBEST for her love, interest, support and motivation.

I would like to thank Melisa YEKE, MSc., Ozan AYAKDAŞ, MSc., and Abdülmecit Harun SAYI, MSc. for their devoted support, guidance and encouraging approach during the learning and writing process of my master's thesis.

Last but not least, I also offer very special thanks to many others who are not mentioned but who have contributed in one way or another to the successful completion of this thesis.

# ABSTRACT


## EXPERIMENTAL ANALYSIS AND MODELING OF SHEAR STRENGTH OF ADHESIVE-BONDED SINGLE-LAP GLASS FIBER REINFORCED COMPOSITES

Composite materials are being used in many fields of industry day by day. With this increasing interest in composites, the methods of joining composites have also become the focus of attention. Mechanical fasteners cause damage to the composite, increase in weight, and stress accumulation in the joint area. Recently, joining composites with adhesives has attracted the attention of researchers.

In this study, glass fiber reinforced polymer composites were combined with two paste adhesive thicknesses, using two brands of paste adhesives as fast-curing and slow-curing, and three different peel plies and the effects of these three different parameters on the bonding strength were investigated both experimental and numerical analyses. In the experimental part of the thesis, glass fiber reinforced polymer composites were produced by the vacuum infusion method. The surfaces modified with different peel plies were combined with two different paste adhesives. A single-impact shear test was performed to examine the bond strength. As a result, it was observed that the fast-curing paste adhesive showed better performance in bond strength. At the same time, it has been experimentally demonstrated that the paste adhesive thickness of 0.6 mm has a positive effect compared to the paste adhesive with a thickness of 0.4 mm. It has been observed that the different peel plies used did not make a critical difference in the bond strength. In the numerical part of the thesis, six different regression models were used to model the shear strength of adhesive-bonded composites and then an optimization study was carried out by selecting the two best regression models that accurately express the physical model. Using the stochastic optimization methods, Differential Evolution and Nelder Mead algorithms, the optimum shear strength values possible with the existing parameters were found. This thesis contributes to determination of the bonded samples with the highest shear stress value by determining the optimum parameters.

# ÖZET

## YAPIŞTIRICI İLE BAĞLANMIŞ TEK BİNDİRMELİ CAM ELYAF TAKVİYELİ KOMPOZİTLERİN KESME DAYANIMININ DENEYSEL ANALİZİ VE MODELLENMESİ

Kompozit malzemeler gün geçtikçe endüstrinin birçok alanında kullanılmaktadır. Kompozitlere olan ilginin artmasıyla birlikte kompozitlerin birleştirme yöntemleri de ilgi odağı haline gelmiştir. Mekanik bağlantı elemanları kompozitin zarar görmesine, ağırlık artışına ve bağlantı bölgesinde stres birikmesine neden olur. Son zamanlarda kompozitlerin yapıştırıcılarla birleştirilmesi araştırmacıların ilgisini çekmiştir.

Bu çalışmada, cam elyaf takviyeli polimer kompozitler, hızlı kürlenen ve yavaş kürlenen olmak üzere iki marka macun yapıştırıcı kullanılarak iki macun yapıştırıcı kalınlığı ve üç farklı soyma katıyla birleştirildi ve bu üç farklı parametrenin yapışma mukavemeti üzerindeki etkileri hem deneysel hem de sayısal analizlerle araştırıldı. Tezin deneysel kısmında cam elyaf takviyeli polimer kompozitler vakum infüzyon yöntemi ile üretilmiştir. Farklı soyma katları ile modifiye edilen yüzeyler iki farklı macun yapıştırıcı ile birleştirilmiştir. Yapışma mukavemetini incelemek için tek darbeli kesme testi yapılmıştır. Sonuç olarak, hızlı sertleşen macun yapıştırıcının yapışma mukavemetinde daha iyi performans gösterdiği gözlemlenmiştir. Aynı zamanda, 0,6 mm kalınlığındaki pasta yapıştırıcının 0,4 mm kalınlığındaki pasta yapıştırıcıya kıyasla olumlu bir etkiye sahip olduğu deneysel olarak gösterilmiştir. Kullanılan farklı soyma katlarının yapışma mukavemetinde kritik bir fark yaratmadığı gözlemlenmiştir. Tezin sayısal kısmında, yapıştırıcı bağlanmış kompozitlerin kayma mukavemetini modellemek için altı farklı regresyon modeli kullanılmış ve ardından fiziksel modeli doğru bir şekilde ifade eden en iyi iki regresyon modeli seçilerek bir optimizasyon çalışması gerçekleştirilmiştir. Stokastik optimizasyon yöntemleri olan Diferansiyel Evrim ve Nelder Mead algoritmaları kullanılarak mevcut parametrelerle mümkün olan optimum kayma mukavemeti değerleri bulunmuştur. Bu tez, optimum parametrelerin belirlenerek en yüksek kayma gerilmesi değerine sahip yapıştırılmış numunelerin belirlenmesine katkı sağlamaktadır.

# TABLE OF CONTENTS

LIST OF FIGURES ..... vii

LIST OF TABLES ..... ix

CHAPTER 1. INTRODUCTION ..... 1
1.1. Introduction Composite Materials ..... 1
1.1.1. Fiber–Reinforced Polymer (FRP) Composites ..... 2
1.2. Vacuum Infusion Method ..... 4
1.3. Bonding of Composites Materials ..... 4
1.4. Surface Treatment with Peel Ply ..... 6
1.5. Objectives of Thesis ..... 6

CHAPTER 2. LITERATURE REVIEW ..... 8

CHAPTER 3. MATERIALS AND METHOD ..... 10
3.1. Materials ..... 10
3.2. Manufacturing of Composites Laminate by Vacuum Infusion Method 10
3.3. Bonding at Composite Laminate ..... 14
3.4. Mechanical Testing ..... 14
3.4.1. Single Lap Joint Test ..... 14

CHAPTER 4. MODELING ..... 17
4.1. Regression Analysis ..... 17
4.1.1. Simple Linear Regression ..... 20
4.1.2. Simple Non-linear Regression ..... 20
4.1.3. Multiple Linear Regression ..... 21
4.1.4. Multiple Non-linear Regression ..... 21
4.2. Coefficient of Determination (R2) ..... 21

CHAPTER 5. OPTIMIZATION ..... 23
5.1 Single Objective Optimization ..... 24

5.2 Multi Objective Optimization ..... 25
5.3 Traditional and Non-Traditional Optimization Methods ..... 26
5.3.1 Nelder-Mead Algorithm ..... 27
5.3.2 Differential Evolution Algorithm ..... 28

CHAPTER 6. RESULTS AND DISCUSSION ..... 30
6.1. Problem Statement ..... 30
6.2. Single Lap Joint Test ..... 30
6.3. Regression Modeling Results ..... 39
6.4. Optimization Results ..... 41

CHAPTER 7. CONCLUSION ..... 44

REFERENCES ..... 46

# LIST OF FIGURES

**Figure** **Page**

Figure 1. Composite materials composition. ..... 1
Figure2. Flowchart of the GFRP matrix composites preparation and characterization ..... 3
Figure 3. Flow chart for optimum design process. ..... 7
Figure 4. Peel Ply Layup on the mold. ..... 10
Figure 5. BIAX1000 Fabrics Layup on the mold. ..... 11
Figure 6. Peel Ply Layup on the fabrics. ..... 11
Figure 7. Green mash is placed on the peel ply. ..... 12
Figure 8. Resin and Vacuum Lines Usage on the mold. ..... 12
Figure 9. 15th minute of the infusion process. ..... 13
Figure 10. 30th minute of the infusion process. ..... 13
Figure 11. 0.4 mm Single lap joints test specimen. ..... 15
Figure 12. 0.6 mm Single lap joints test specimen. ..... 16
Figure 13. Top view of Bonded test specimen. ..... 16
Figure 14. Side view of Bonded test specimen. ..... 16
Figure 15. Flow diagram for the optimal design. ..... 17
Figure 16. Steps of regression analysis. ..... 18
Figure 17. Regression Graph for Simple Linear Model. ..... 20
Figure 18. The minimum and maximum of the objective function f (x). ..... 24
Figure 19. Nelder-Mead algorithm flowchart. ..... 28
Figure 20. Flowchart of Differential Evolution Algorithm ..... 29
Figure 21. Single lap joints test ..... 31
Figure 22. Single Lap Joint Test Load-Extension Diagram of Adsh-1-Nylon-0.4 ..... 31
Figure 23. Single Lap Joint Test Load-Extension Diagram of Adsh-2-Nylon-0.4. ..... 32
Figure 24. Single Lap Joint Test Load-Extension Diagram of Adsh-1-Nylon-0.6 ..... 32
Figure 25. Single Lap Joint Test Load-Extension Diagram of Adsh-2-Nylon-0.6. ..... 33
Figure 26. Single Lap Joint Test Load-Extension Diagram of Adsh-1-PA-0.4. ..... 33
Figure 27. Single Lap Joint Test Load-Extension Diagram of Adsh-2-PA-0.4. ..... 34
Figure 28. Single Lap Joint Test Load-Extension Diagram of Adsh-1-PA-0.6. ..... 34
Figure 29. Single Lap Joint Test Load-Extension Diagram of Adsh-2-PA-0.6. ..... 35

**Figure** **Page**

Figure 30. Single Lap Joint Test Load-Extension Diagram of Adsh-1-Green-0.4 ..... 35
Figure 31. Single Lap Joint Test Load-Extension Diagram of Adsh-2-Green-0.4 ..... 36
Figure 32. Single Lap Joint Test Load-Extension Diagram of Adsh-1-Green-0.6..... 36
Figure 33. Single Lap Joint Test Load-Extension Diagram of Adsh-2-Green-0.6..... 37
Figure 34. Single Lap Joint Test Results. ..... 37
Figure 35. After test images of single lap joints test specimens..... 39

# LIST OF TABLES

**Table** **Page**

Table 1. Regression models types including linear, quadratic, trigonometric, logarithmic, and their rational forms ..... 19
Table 2. Materials Description..... 30
Table 3. The Average Shear Stress (MPa) Results of Test Samples ..... 39
Table 4. Mathematical functions observed from regression analysis ..... 40
Table 5. Fit and boundedness check of the regression models..... 41
Table 6. Results of the optimization problems for Shear Stress..... 42
Table 7.Results of the optimization problem for Differential Evolution and Nelder Mead Model according to Target 16 MPa ..... 43

# CHAPTER 1

# INTRODUCTION

## 1.1. Composite Materials

Although the use of composite materials is not as common in the industry as the use of metal materials, it is in demand in many areas of the industry. Composite material is formed by combining two significantly different structures or more than two materials in specified proportions and if they meet the desired conditions. If we examine the substances in composite materials, there are two different substances. Matrix and reinforcement material. The physical properties of these materials are different from each other [1]. The matrix material serves to hold the fibers together, transfers the load on the material to the fibers protects the material against external damage, gives the material its shape, and keeps the material hard [1]. The Reinforcement Material acts as the carrier, and the matrix phase around it serves to hold and support it together (Figure 1).

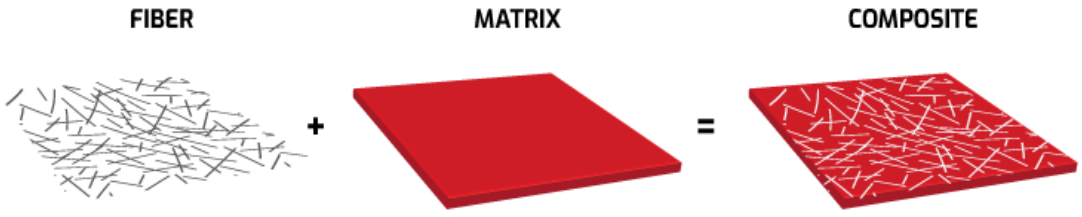


Figure 1. Composite materials composition.
(Source: https://romeorim.com/what-are-composites/)

The first known usage of composites is credited to Mesopotamians. They created plywood by joining wood at certain angles [1]. Mesopotamians combined wood sawdust and natural resin. As a result, chipboards were obtained. Later, the Mongols used springs obtained from plants, pine resin, animal tendons and horns as examples of composite uses in history [1].

When we look at the usage areas of composites, we see that composites have very wide application areas in the aviation industry. Composite materials find applications in interior design and the production of structural materials in airplanes and helicopters, leveraging their superior mechanical properties while maintaining a

lightweight profile. In the construction industry, materials with diverse internal structures are employed, and these structures must possess the desired properties for optimal performance. Facade protection, holiday homes, buffets, bus stops, cold storage, and construction molds are composite material applications. The purpose of using composites in the automotive industry is to lighten the skeleton of the vehicle and increase impact resistance. Another area where composites are widely used is the healthcare field. In orthopedics, composite materials are used as internal and external connection systems for broken bone repair, when necessary. In dentistry, composite resins are used as dental fillings and epoxy resin reinforced with collagen fibers is used as dental support material [1].

### 1.1.1. Fiber–Reinforced Polymer (FRP) Composites

In areas such as automotive, construction, and sports industries, natural fibers stand out with their features such as low cost, low density, low energy input, and comparable mechanical properties.

Currently, most automobile factories use natural fiber composites in the materials of their interiors, door coverings, and panels. Wood fibers are also used in the seats. In addition, cotton fibers are used as sound insulation material. To reduce the weight of the cars, polyurethane was used in the door coverings, and the reinforcement was done with a linen/sisal blend mat [1]. The depiction of the preparation and characterization of composites with a Glass Fiber Reinforced Polymer matrix is presented in Figure 2. Fiber-reinforced materials have emerged as a significant class of structural materials, often preferred over metals in many weight-critical components in industries such as aerospace and automotive.

A fiber-reinforced composite (FRC) is a building material composed of three components: fibers as the dispersed phase, a matrix as the continuous phase, and the interphase region, also known as the interface. This material is used in construction due to its strength and durability.

Unlike other composites, this material can be recycled up to 20 times, allowing for the reuse of scrap FRC.

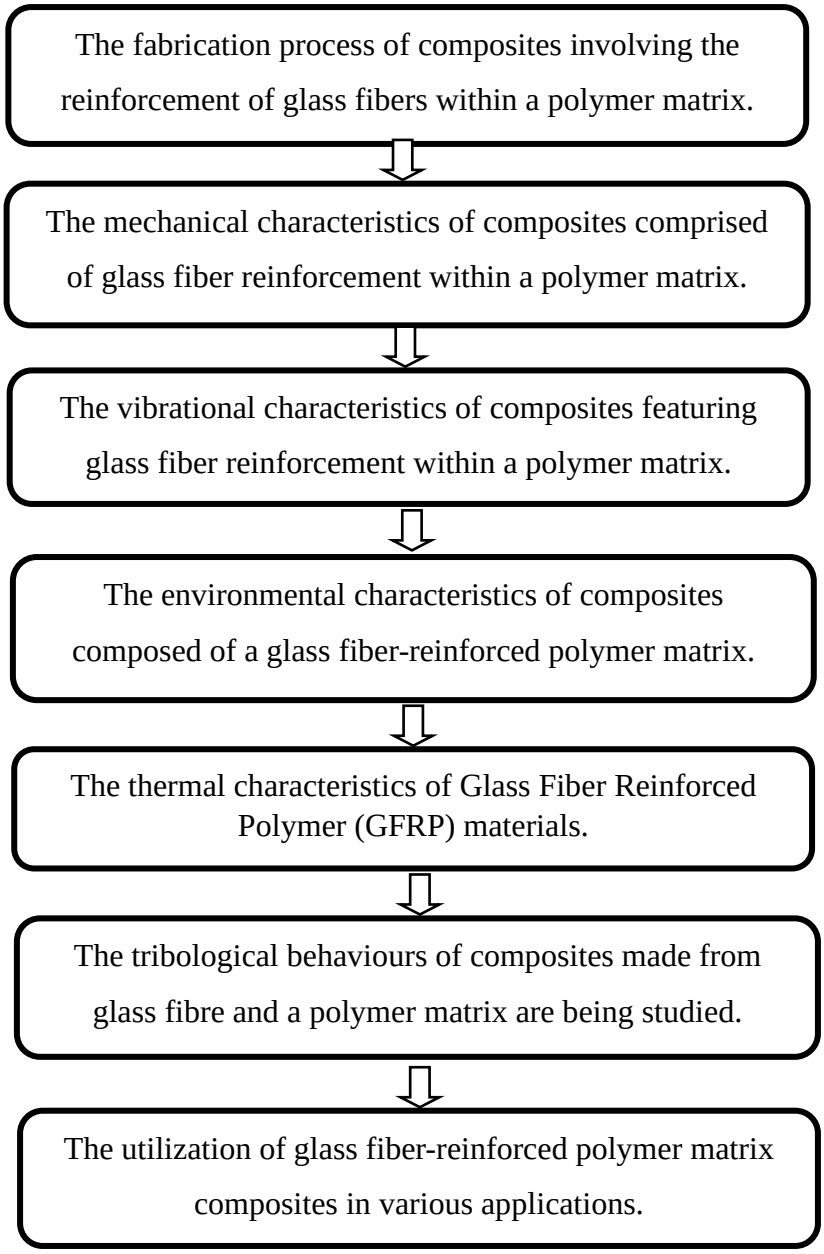


Figure 2. Flowchart of the GFRP matrix composites preparation and characterization[2].

Failure mechanisms in FRC materials include delamination, intralaminar matrix cracking, longitudinal matrix splitting, fiber/matrix debonding, fiber pull-out, and fiber fracture.

## 1.2. Vacuum Infusion Method

The vacuum infusion technique has been used especially in the USA since the 1980s. It is a material production method used in various industrial sectors around the world. This method is based on the principle of movement of resin in a vacuum environment, and production is aimed without human intervention at the point where the manufacturing stages of the product are completed [1]. This innovative technique is often used for the production of composite parts with complex structures, and the appropriate viscosity of the resin impregnated into the materials is important. In narrow spaces and long flow paths, it is necessary for the resin to penetrate the reinforcement fibers as quickly as possible.

Although the general system of the infusion technique is the same, application methods may vary. The infusion technique consists of four main parts: vacuum pump, vacuum tank (resin collection tank), mold, and resin bucket. The connections and shapes of these four parts may vary, but the basic system logic is always constant [3]. There are two different vacuum infusion processes and the place where the resin enters the mold varies in these processes.

## 1.3. Bonding of Composite Materials

Adhesive bonding is a material joining process in which the adhesive between two surfaces solidifies, forming an adhesive bond [4].

Recently, it has been observed that adhesive bonding management has been used instead of the currently used joining methods. The reason for this is its high strength/weight ratio, usability of its design, damage tolerances, fatigue resistance, etc. This combination method is used because it is more convenient in many aspects, such as. There are various areas where adhesive bonding management is used. These fields are aviation, automobile, sports, electronics, maritime, oil, and construction fields.

There are adhesive bonding applications for the repair of composites in damaged structures in these sectors [1].

In 2009, Banea and da Silva conducted a study on parts assembled by adhesive composite materials. After these dates, studies on composite materials have increased [5].

The assembled part connections are generally not expected to hurt the load-carrying capacity of the structures. These connections are expected to withstand static or cyclic loads for a long time. The lack of optimum material models and failure criteria has resulted in a tendency to 'over-design' composite structures. Often safety considerations require that adhesive-bonded structures, primarily those used in primary load-bearing applications, additionally include mechanical fasteners (e.g. bolts) as a safety measure [1].

Some reasons why adhesive bonding is much preferred compared to different bonding methods are given below.

1. It can generally be used in thinner impression materials to save cost and weight.

2. Reducing the number of production parts can simplify the design.

3. There is less need for milling or shaping for fine details.

4. Large volume connections can be made with less labor, without requiring special skills.

5. Adhesive bonding offers a high strength-to-weight ratio, providing approximately three times the shear force compared to riveted joints.

6. Improved visual appearance is achieved through enhanced aerodynamic smoothness.

7. Electrical and thermal insulation is very good.

8. Adhesive-joined assemblies demonstrate superior fatigue resistance, with a fatigue life approximately twenty times better than riveted structures composed of identical parts.

9. Damping properties and noise reduction are better than riveted assemblies.

10. It is flexible enough to allow changes in thermal expansion coefficients when joining different materials.

While adhesive bonding presents numerous advantages, it is crucial to have methods for analyzing, designing, and optimizing adhesive bonding joints for various configurations under multiple load conditions. [6].

## 1.4. Surface Treatment with Peel Ply

Roughness of adherend surfaces has frequently been used as a design parameter for adhesive joints. To ensure a stronger and more durable connection between two different surfaces, a prior surface treatment is required. Specific parameters expected to be improved by these surface treatments are roughness, chemical modification, surface free energy, etc.

There are the following surface treatment techniques that act by roughening the surface. For example, sandblast, solvent etching, peel ply, and laser treatment methods such as plasma are used [7]. Besides, modelling and optimization of the material were performed using Regression approach and statistics optimization methods.

Peel Ply application is one of the most used processes in the composite industry. The main reason for this is its low cost and ease of use. However, due to its industrial use in very competitive fields, only a few complete studies on this topic have been reported in the literature [8,9].

## 1.5. Objectives of Thesis

Owing to the numerous benefits that composite materials offer; their use is growing daily. The excellent strength, low weight, high corrosion resistance, and fatigue resistance of fiber-reinforced structural composite parts are particularly encouraging in the aviation industry. The connecting of these pieces has gained attention as the focus shifts to fiber-reinforced structural composite parts. Weight growth, delamination, and stress buildup around the fastener are among the major issues that fiber-reinforced composite parts united using traditional techniques lead to. Furthermore, corrosion and negative electromagnetic characteristics are caused by these metallic connection parts, such as rivets and screws. This is why one of the cutting-edge bonding methods, paste adhesives, is becoming more and more popular. But in order to accomplish this, surface alteration is needed.

In this study, composite materials were obtained with 10 layers of BIAX1000 fabric. Three composite materials with different surface roughness were made by using

three different peel plies on the surfaces of the resulting composite materials. These materials were bonded to each other with two different paste adhesives coded as EPIKOTE Adhesive 1 and EPIKOTE Adhesive 2. These materials are bonded to each other in two different thicknesses: 0.4 mm and 0.6 mm.

The main aim of the study is to design the material with the best mechanical performance among the composite materials bonded to each other with different roughness, different paste adhesives, and different paste adhesive thicknesses. Single Lap Joint (SLJ) tests were performed to examine mechanical property characterization. Additionally, modeling and optimization of adhesive-bonded single-lap glass fiber reinforced composites for maximum shear strength were performed using the defined regression models and stochastic optimization methods such as Differential Evolution(DE) and Nelder Mead(NM). The flowchart of the optimization study is summarized in Figure 3.

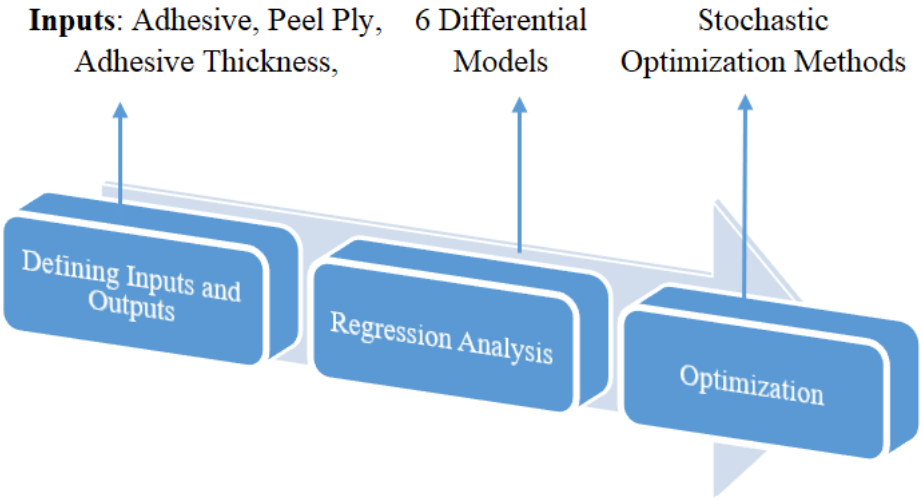


Figure 3. Flow chart for optimum design process

# CHAPTER 2

# LITERATURE REVIEW

Composite materials have started to be used in the aviation, defense sector, and wind turbine manufacturing because they have the characteristics of high specific strength, lightweight material, and low production time. For this reason, interest in the research of these materials has increased. Fiber-reinforced fabrics exhibit notable advantages, including robust corrosion resistance, reduced weight, and enhanced fatigue strength, rendering them superior to commonly utilized materials like metals. Various alternatives have been used to bond composite materials to each other. Adhesive bonding is one of the most common methods. Adhesive bonding is a material joining process in which the adhesive between two surfaces solidifies, forming a cohesive bond. Adhesion thickness is one of the important factors. While these are bonded, the roughness of the bonded surfaces is also important. Recent literature focuses on the factors that connect two composite materials in mechanical connections.

Hanumantharaya Rangaswamy et al. They examined the damage behaviour of adhesive-bonded joints. They found that these damage behaviours were largely affected by geometric parameters (adhesive thickness and overlap length) and bonded surface preparations. Single lap adhesive connections were prepared to find the strength of glass fiber reinforced epoxy composites with different geometric factors. The two bonded composite surfaces were roughened. Taguchi L9 experimental matrix, comprising various combinations of lap lengths and adhesive thicknesses, was employed to investigate the behavior of damage load (FL) and shear strengths (SS) in adhesive-bonded single-lap composite joints. As a result, these studies showed that the effect of the overlap length of assembled joints is greater than the adhesive thickness. Separate empirical relationships for fracture load and shear strength were derived using multiple linear regression (MLR) equations.Neural networks (NNs) trained with the Levenberg-Marquardt algorithm were used to predict both responses. Both MLR and NN were checked for their prediction abilities with ten experimental cases [10].

Mojtaba Hassan Vand et al. investigated the optimization of the stacking order of composite laminate bonded parts. In doing so, they aimed to minimize the amount of peeling and shear stress of an adhesive layer. In the study, the effects and results of different assumptions on stress equations are presented. Optimization results showed

that the maximum shear and peel stress strongly depend on the extension, joint, and bending stiffness, such that the bonded parts in the optimum model have high and almost equal stiffness. In the worst scenario, there is a large difference in the hardness of the bonded parts, causing devastating high stress in the thinner bonded part [11].

Grant L. and Al. These studies were conducted to determine the effect of using adhesives instead of spot welding in automobile production. Testing and finite element analysis were performed using various loadings. Lap joints were tested under tension (producing shear along the bond line), three-point loading (bending plus shear), and four-point loading (pure bending). Various parameters such as overlap length and tie line were investigated. It was concluded that the three-point bending and tensile loads were very similar in terms of affecting the adhesive, while the four-point bending test didn't cause failure because the steel yielded before the connection broke. A criterion for damage is proposed based on the tensile load and bending moment applied to the connection [1] .

Mehmet Erdem İriş conducted research on adhesive joints and found that while they have advantages over mechanical joining, there are many parameters that can affect adhesion quality, making the joining process more complicated. In this study, the effects of these parameters on adhesion quality were examined comprehensively and a study was conducted to guide designers and researchers [12].

Ferhat Kadıoğlu conducted research on connection behavior under quasi-static buckling conditions. The study tested joints with three different adhesive thicknesses and a 25 mm overlap length, using two different adhesive types and an adhesive film. The joints were modelled using a non-linear Finite Element Method implemented through the ABAQUS Explicit package. The study identified critical stresses in compression during buckling mode and in peeling during the tensile mode. The research emphasised the crucial role of adhesive mechanical properties in connection performance [13].

Levent Aydin et al. employed a multi-objective optimisation approach to determine the number of low-cost layers with high stiffness needed to achieve a lightweight and low-cost design with maximum natural frequency. This study is the first in the literature to investigate the optimisation problems of natural frequency-price and natural frequency-weight of flax,a natural fibre,for layered composite plates.It optimizes frequency, price, and weight without compromising the specific stiffness ratio [1].

# CHAPTER 3

# MATERIALS AND METHODS

This chapter explains the materials used and the production stages of the test sample parts. The description of the bonding of the test specimens will follow.

## 3.1. Materials

In this study, BIAX1000 fabric was used to produce composite materials. Two types of EPIKOTE adhesives were used to join the composite materials. The density of the first adhesive of these materials is 1.10 - 1.15 g/cm3, and the density of the second adhesive is 1.15 - 1.25 g/cm3. To obtain the surface roughness, 3 different peel plies were used: FLOGREEN, Nylon Peel Ply, PA66 PA6 85R. These materials weight 85 g/m2, 92 g/m2, 80 g/m2, respectively.

## 3.2. Manufacturing of Composites Laminate by Vacuum Infusion Method

Composite production of 10 layers of BIAX 1000 fabrics has been realized. This production was carried out with vacuum infusion management. The following steps were followed while producing the samples using the vacuum infusion method.

Step 1) Scratches, dust, etc. on the mold surface. Foreign substances were cleaned from the mold surface. A peel ply was laid at the bottom to ensure surface roughness (Figure 4).

Figure 4. Peel Ply Layup on the mold

Step 2) 10 layers of BIAX fabrics were placed on top of each other, and a bond was sprayed between them to prevent the fabrics from slipping. The fabrics were cut and laid out in 100*50 cm dimensions to fit the pattern. This process is presented in Figure 5.

Figure 5. BIAX1000 Fabrics Layup on the mold

Step 3) After the fabric laying was completed, peel ply was laid on the entire mold to ensure surface roughness and it was adhered to the fabrics with adhesive. This process is presented in Figure 6.

Figure 6. Peel Ply Layup on the fabrics

Step 4) In order to ensure the advancement of the resin, a green mash is placed on the peel ply at the top (Figure 7).

Figure 7. Green mash is placed on the peel ply

Step 5) Sealing was ensured by applying infusion paste tape to the edges of the vacuum foil. Resin and vacuum lines are adjusted according to the surroundings of the mold. This process is presented in Figure 8.

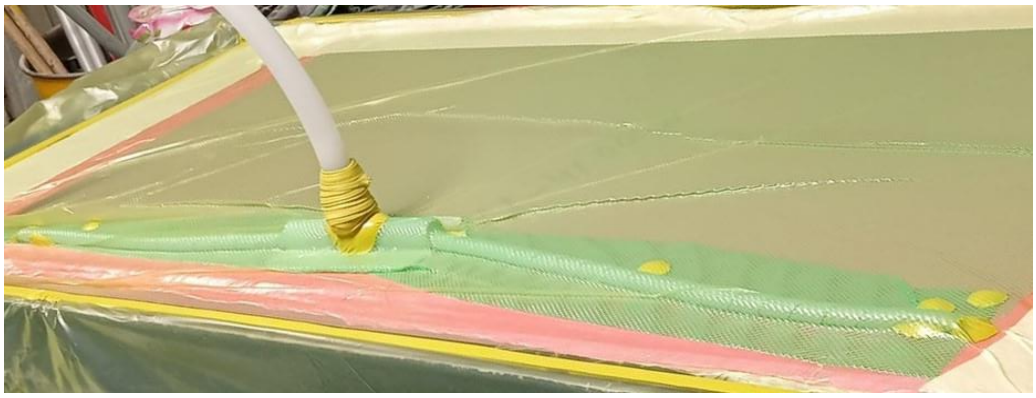

Figure 8. Resin and Vacuum Lines Usage on the mold

Step 6) A vacuum gauge is connected to the vacuum infusion device and the vacuum pump is turned on. The vacuum bag was checked for leaks using a vacuum gauge and leak detector.

Step 7) Ports that will allow resin passage are connected to the mechanism. The required amount of resin has been prepared. As seen in Figure 8. the hoses were connected to the ports and the resin flow started. The process continued until every point of the mold was wet with resin. Finally, the corners of the mold got wet. After all points were wetted, all resin supply lines were clamped. The infusion flow proceeded as in Figure 9.

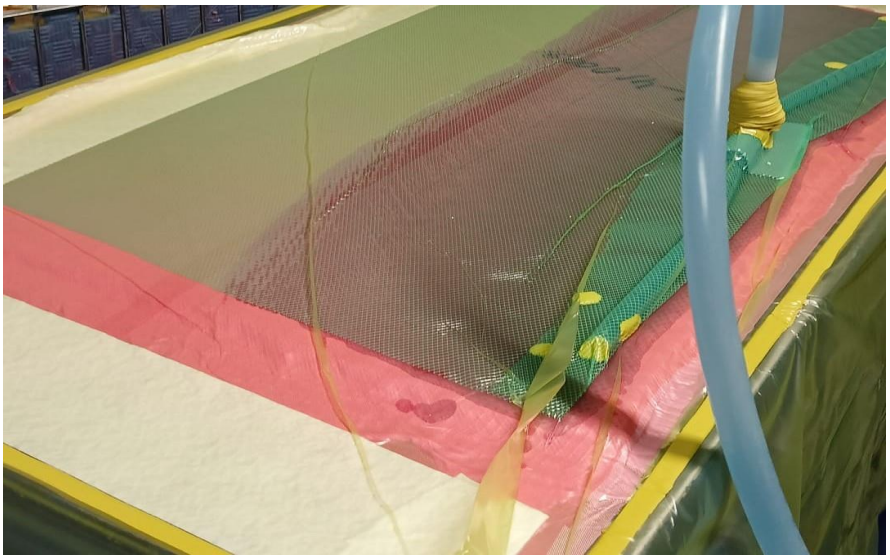

Figure 9. 15th minute of the infusion process

Step 8) As seen in Figure 10. , the part was kept under vacuum until it completely hardened. The sealing tape was separated, and the vacuum foil was removed from the mold. The infusion resin wetted the entire fabric as in Figure 9.

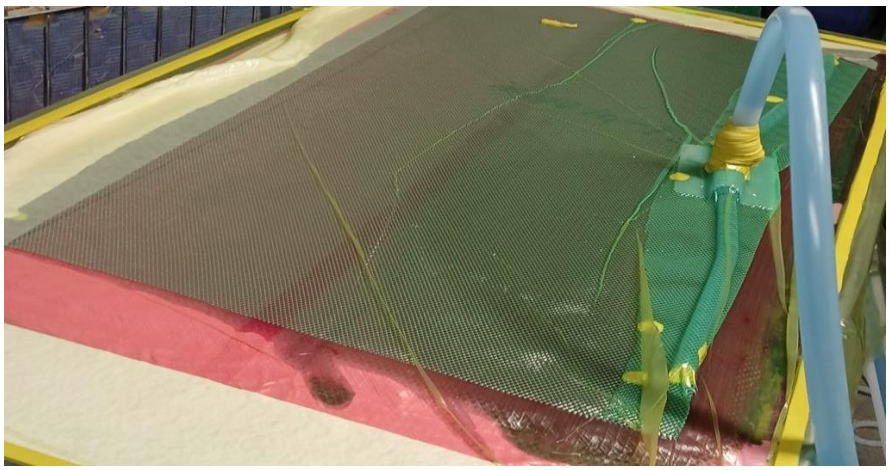

Figure 10. 30th minute of the infusion process

Step 9) The part was then removed from the mold.

## 3.3. Bonding at Composite Laminate

All mechanical test samples were prepared by cutting them on a vertical cutting machine according to the ASTM 5868-01 test standard. Before preparing the samples, the edges of the composite plates were cut approximately 25 mm. Preparing the test samples from the middle of the composite plate ensured more homogeneous and realistic preparation. The cut samples were bonded to each other.

Two different paste adhesives were applied in two different thicknesses, 0.4 mm, and 0.6 mm, to the joint areas where Peel Ply was applied. EPIKOTE adhesive 1, adhesive was cured for 4.2 hours at 70 degrees. EPIKOTE adhesive 2, adhesive was cured in 3.5 hours.

## 3.4. Mechanical Testing

Mechanical tests were carried out on the bonded samples prepared according to the ASTM 5868-01 test standard on the MTS Landmark Servohydraulic Testing Machine for Single Lap Joint Test (SLJ).

### 3.4.1. Single Lap Joint Test (SLJ)

As designers and engineers persist in extending the limits of high-performance design, the use of Fibre Reinforced Plastics (FRP) is becoming more and more common. FRP is especially preferred in structural applications because it has lightweight and has superior mechanical properties. Applications, particularly in the aerospace and automotive industries, frequently demand geometric complexity, the integration of multiple components, and the joining of dissimilar materials. These requirements result in the need for assembly and joining elements (usually mechanical fasteners or adhesives). Adhesive bonding is frequently the preferred method for fabricating Fiber-Reinforced Polymer (FRP) structures, as it eliminates the need for material removal, thereby reducing stress concentrations and the risk of stress cracking [14,15].

Compared to mechanical fasteners, adhesive bonding provides an advantage by not causing stress concentrations and stress cracking that occur during drilling and

assembly. Additionally, adhesive bonding supports the lightweight design goal and reduces maintenance costs by reducing galvanic corrosion. Adhesive bonds are typically engineered to function under shear loads, wherein forces act in opposing directions parallel to the plane of the adhesive. Tensile shear testing is commonly used to determine this condition. However, one of the difficulties encountered in this test is the complex loading conditions at the adhesive-adhesive interface, which can affect the results and lead to misleading conclusions [16,17].

Modified and unmodified glass fiber plates in the joint area were bonded with EPIKOTE adhesive 1 and EPIKOTE adhesive 2, adhesives. Single Lap Joints Test was applied to determine the shear strength of the adhesive. The tests were carried out in the IZTECH laboratory using the MTS Landmark Servohydraulic Test System. Test coupons were prepared according to ASTM D5868-01 standard. The test was performed at a speed of 13 mm/min. Figure 11 shows the dimensions of the 0.4 mm thick Single Turn Joint Test sample and the dimensions of the 0.6 mm thick Single Lap Joint Test sample is given in Figure 12.

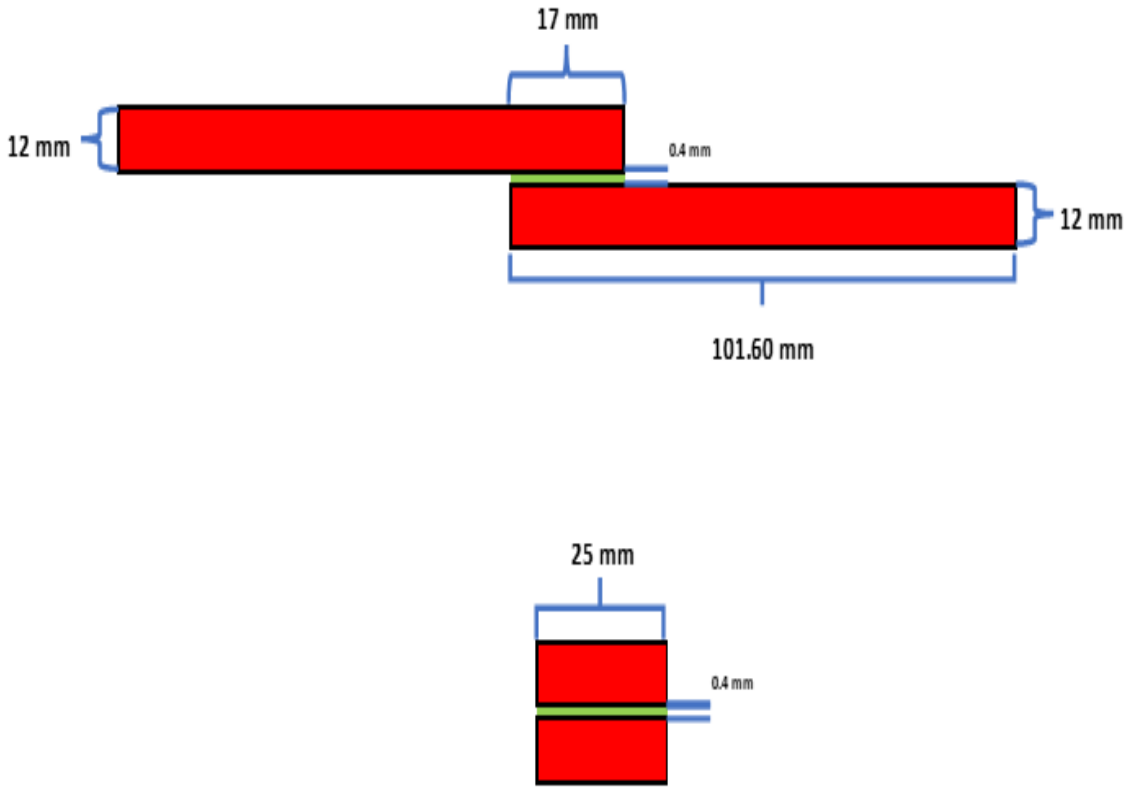


Figure 11. 0.4 mm Single lap joints test specimen

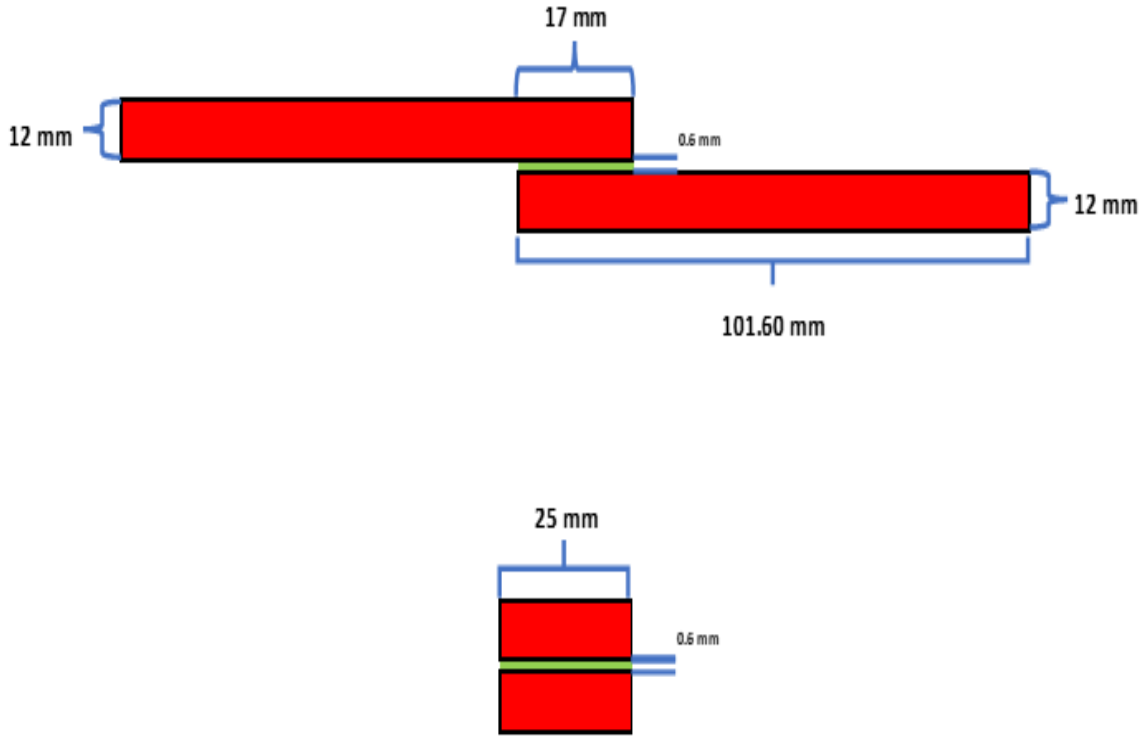


Figure 12. 0.6 mm Single lap joints test specimen

The samples to be tested were bonded to each other with paste adhesive. The top view of the samples is seen in Figure 13.


Figure 13. Top view of bonded test specimen

The side view of the test sample is shown in Figure 14. In order for the samples to have a thickness of 0.4 mm and 0.6 mm, shims of 0.4 and 0.6 mm thickness were placed between the two samples.

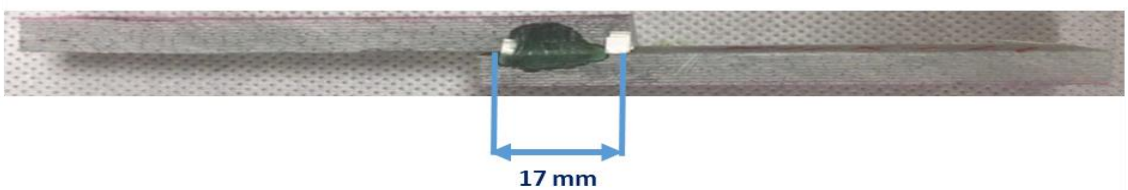


Figure 14. Side view of bonded test specimen

# CHAPTER 4

# MODELING

A model is a representation of idea simplification and reflection of a real-world system or occurrence. The process of modeling involves making an unknown event understandable and visible by utilizing information from existing sources. In its widest sense modeling is the act of reproducing reality. Additionally, modeling is a method used in making abstract mathematics more concrete. Within this context, mathematical modeling is a dynamic approach that helps in discovering connections in real-life situations pressing them mathematically categorize drawing conclusions. [18,19]

Models which are commonly used in engineering challenges are small structures that represent larger systems. These models effectively capture the characteristics and intended applications of the system. In the advancement of optimization technologies, academics have placed significant emphasis on modeling, with mathematical modeling serving as the initial step in optimizing engineering design problems. The mathematical models are developed using experimental or simulation data and include quantifiable characteristics of the systems, design factors that determine the performance standards to be optimized and constraints that establish their limits[20]. Figure 15 outlines the process of designing a system starting with the development of an experiment and ending with the identification of the optimal solution.

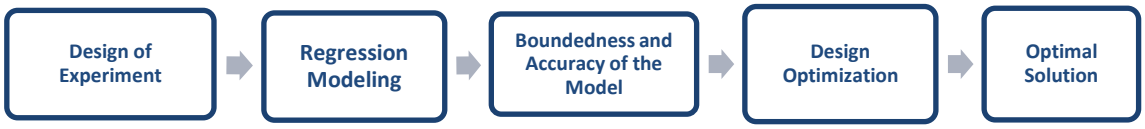


Figure 15. Flow diagram for the optimal design [21]

Within this thesis, data for the experiment were obtained by using the Regression Analysis, which is used in order to carry out the modeling optimization.

## 4.1. Regression Analysis

Regression is a widely used statistical method for investigating cause-and-effect relationships among two or more variables. Essentially, it involves examining how one or more variables influence others. The relationship between these variables is represented as a mathematical function, termed a regression function or a regression

model. In the regression model, the dependent variable (response variable) is denoted as Y, while the independent variables (design variables) are denoted as $X_i$ (i=1, 2,..,n). Depending on the number of variables used and the type of model, regression analysis can be categorized into simple linear regression, simple nonlinear regression, multiple linear regression, and multiple nonlinear regression. Regression analysis steps are given in Figure 16.

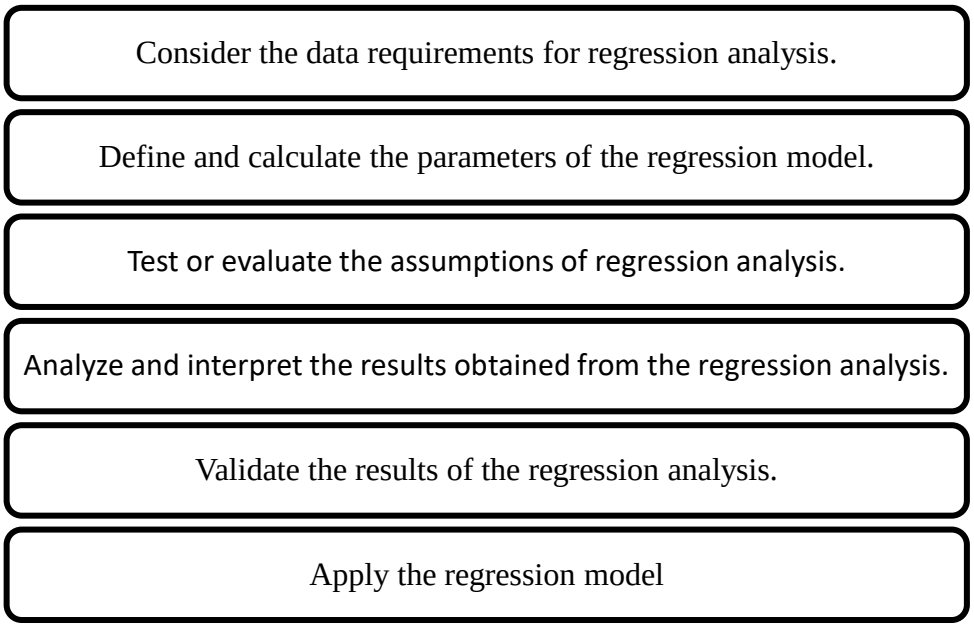


Figure 16. Steps of regression analysis

Regression analysis is one of the basic techniques used to prove the accuracy of models, make preliminary predictions about their parameters, and test them. In order to obtain the best results, twelve different mathematical models were tested in optimization. The names and formulas of the mathematical models applied in the modeling study are given in Table 1.

Generally, a regression model is expressed by Equation 1 (y represents the dependent variable, α represents the constant, x1 represents independent variable, β1 indicates the (regression) coefficient of the independent variable x and the e denotes the error (or residual) of the equation) .

$$y = a + \beta_1 X_1 + \in \quad (1)$$

Table 1. Regression models types including linear, quadratic, trigonometric, logarithmic, and their rational forms

| Model Name | Nomenclature | Formula |
|---|---|---|
| Multiple linear | L | $Y = \sum_{i=1}^{2}(a_i x_i) + c$ |
| Multiple linear rational | LR | $Y = \frac{\sum_{i=1}^{2}(a_i x_i) + c_1}{\sum_{j=1}^{2}(\beta_j x_j)} + c_2$ |
| Second order multiple non-linear | SON | $Y = \sum_{k=1}^{2}\sum_{j=1}^{2}(a_j x_j x_k) + \sum_{i=1}^{2}(a_i x_i) + \ c$ |
| Second order multiple non-linear rational | SONR | $Y = \frac{\sum_{k=1}^{2}\sum_{j=1}^{2}(a_j x_j x_k) + \sum_{i=1}^{2}(a_i x_i) + \ c_1}{\sum_{l=1}^{2}\sum_{m=1}^{2}(\beta_m x_m x_l) + \sum_{n=1}^{2}(\beta_n x_n)} + c_2$ |
| First order trigonometric multiple non-linear | FOTN | $Y = \sum_{i=1}^{2}(a_i Sin[x_i] + a_i Cos[x_i]) + c$ |
| First order trigonometric multiple non-linear rational | FOTNR | $Y = \frac{\sum_{i=1}^{2}(a_i Sin[x_i] + a_i Cos[x_i]) + c_1}{\sum_{j=1}^{2}(\beta_j Sin[x_j] + \gamma_j Cos[x_j])} + c_2$ |
| Second order trigonometric multiple non-linear | SOTN | $Y = \sum_{i=1}^{2}(a_i Sin[x_i] + a_i Cos[x_i]) + \sum_{j=1}^{2}(\beta_j Sin^2[x_j] + \gamma_j Cos^2[x_j]) + c$ |
| Second order trigonometric multiple non-linear rational | SOTNR | $Y = \frac{\sum_{i=1}^{2}(a_i Sin[x_i] + a_i Cos[x_i]) + \sum_{j=1}^{2}(\beta_j Sin^2[x_j] + \gamma_j Cos^2[x_j]) + c_1}{\sum_{k=1}^{2}(\theta_i Sin[x_k] + \theta_i Cos[x_k]) + \sum_{l=1}^{2}(\delta_j Sin^2[x_l] + \delta_j Cos^2[x_l])} + c_2$ |
| First order logarithmic multiple non-linear | FOLN | $Y = \sum_{i=1}^{2}(a_i Log[x_i]) + c$ |
| First order logarithmic multiple non-linear rational | FOLNR | $Y = \frac{\sum_{i=1}^{2}(a_i Log[x_i]) + c_1}{\sum_{j=1}^{2}(\beta_j Log[x_j])} + c_2$ |
| Second order logarithmic multiple non-linear | SOLN | $Y = \sum_{k=1}^{2}\sum_{j=1}^{2}(a_j Log[x_j x_k]) + \sum_{i=1}^{2}(a_i Log[x_i]) + c$ |
| Second order logarithmic multiple non-linear rational | SOLNR | $Y = \frac{\sum_{k=1}^{2}\sum_{j=1}^{2}(a_j Log[x_j x_k]) + \sum_{i=1}^{2}(a_i Log[x_i]) + c_1}{\sum_{m=1}^{2}\sum_{l=1}^{2}(a_l Log[x_l x_m]) + \sum_{n=1}^{2}(a_n Log[x_n])} + c_2$ |

### 4.1.1. Simple Linear Regression

The main objective of simple linear regression is to determine the impact of a single-unit alteration in the independent variable on the dependent variable. Its primary aim is to discover a linear equation that illustrates the connection between the dependent and independent variables. Equation 2 expresses a simple linear regression equation, which is a stochastic (probability) model that shows the relationship in the population.;

$$an\ Y = \beta_0 + \beta_1 X + \in \quad (2)$$

Here, $\beta_0$ is the point where the line intersects the y-axis and is the regression constant. If $\beta_1$ is the slope of a straight line or the regression coefficient, $\in$ is a random error value and that error value is assumed to have a normal distribution with zero mean variance $\sigma_2$. This assumption is necessary for the significance testing of coefficients, not for parameter estimates. Figure 17 represents this formula graphically [22].

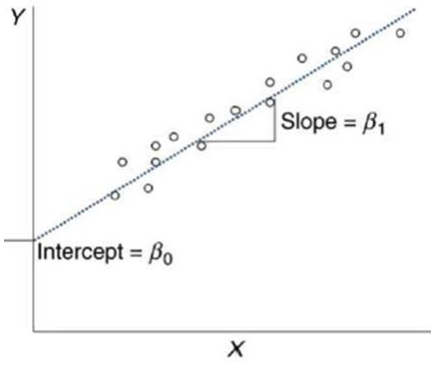


Figure 17. Regression Graph for Simple Linear Model
(Source: H. İ. Erten, 2021) [23]

### 4.1.2. Simple Non-Linear Regression

Simple non-linear regression fits a curve to non-linear X and Y data. Y is a function of one variable x: Y = f (X). Various functions lead to different curves depending on the shape of the data. A basic nonlinear regression for a model with just one input variable is expressed as Equation 3.[24].

$$an\ Y = \beta_0 + \beta_1 X^2 + \in \quad (3)$$

### 4.1.3. Multiple Linear Regression

Simple linear regression analysis examines the connection between a dependent variable and a single independent variable, while multiple linear regression analysis investigates the relationship between a dependent variable and two or more independent variables. Both analyses assume a linear relationship between variables. The general form of the multiple linear regression model is presented in Equation 4.

$$the\ Y = \beta_0 + \beta_1 X_1 + \beta_2 X_2 + \cdots + \beta_n X_n + \in \quad (4)$$

### 4.1.4. Multiple Non Linear Regression

The multiple nonlinear regression model provides a more versatile approach compared to simple nonlinear regression models, as it doesn't require the function to be linear or linearized. Therefore, the nonlinear regression model offers a wide range of options to fit the data. The shape of nonlinear regression models is generally similar to linear regression models. N – the relationship between the number of regression parameters and the quantity of independent variables in the model, meaning X, is the biggest difference that distinguishes the non-linear regression model from the linear regression model. Multiple nonlinear regression was used for analysis in this thesis. The general form of the multiple non-linear regression model is presented in Equation 5.

$$Y = \beta_0 + \beta_1 X_1 + \beta_2 X_2^2 + \cdots + \beta_n X_n^n + \in \quad (5)$$

## 4.2. Coefficient of Determination ($R^2$)

In regression analysis, the commonly used coefficient of determination (R2) is used to see how close the data is to precision. In other words, it shows us the percentage of the changes occurring in the dependent variables that can be explained by the independent variables. Explanatorily, it refers to the regression model. With this value obtained, regression models are calculated as the square of the multiple correlation coefficient. Although this R-squared value is defined as the square of an expression, in some special cases it can be calculated as negative. Given these results, this model is not

reliable. There may be situations where the independent variable cannot explain the dependent variable at all. Here, the coefficient of determination may be zero. This is a sign that he can explain the topic fully. Here zero means 0% of the model, while one means the model has 100% explanatory power. It is recommended that this value be close to 1. Although there is no clear power, the R-square value is expected to be around 0.90 for good modeling. The R-squared formulation is given in equations 6 – 8.

$$R^2 = 1 - \frac{SSE}{SST} \tag{6}$$

$$\text{over}SSE = \sum_i (\hat{y}_i - \bar{y})^2 \tag{7}$$

$$SST = \sum_i (y_i - \bar{y})^2 \tag{8}$$

where,

**SS**E is the Sum of Squared Regression also known as variation explained by the model

**SS**T is the Total Variation in the data also known as the sum of the squared total

$\mathbf{y_i}$ is the y value for observation i

$\bar{\mathbf{y}}$ is the mean of the y value

$\hat{\mathbf{y}}_\mathbf{i}$ is the predicted value of y for observation i

R-squared measures the rate of change in our dependent variable (+Y) that can be explained by our independent variables (X) for a linear regression model. Furthermore, the adjusted R-squared only measures the rate of change explained by the independent variables that affect the dependent variable. The value of $R^2$ is always greater than the set values of $R^2$. According to the non-significant variable added to the model, the $R^2$-corrected value also changes depending on Equation 9.

$$R^2_{adjusted} = 1 - \frac{(1-R^2)(n-1)}{n-k-1} \tag{9}$$

In this equation, k refers to the number of independent regressors, which is the number of variables without a constant in the model, while n represents the number of points in the data sample[24,25], [26].

# CHAPTER 5

# OPTIMIZATION

Optimization is a mathematical process that seeks to find the most efficient design by minimizing or maximizing specific objective functions. It determines the decision variables within the constraints of the problem. In simple terms, optimization finds the inputs or values that will achieve the desired outcome. However, simply finding a solution does not guarantee the best results. That's why optimization techniques are used to identify the optimal solution for the problem at hand. This optimal solution is also known as the best possible outcome. Regardless of the specific problem, the ultimate goal of optimization is to find the optimal solution. This is why optimization is commonly used in engineering problems that involve factors such as mass displacement force time temperature bending stiffness and vibration. [27,2829].

The process of optimization can be divided into two main stages: mathematical modelling and analysis. Mathematical modeling involves translating the characteristics of real-life phenomena into mathematical language. Analysis the other hand involves examining and adjusting the mathematical model to fit real-life situations. Essentially bridges the gap between design variables and objective functions by providing physical interpretation and applying mathematical concepts. [30]

The optimization process can be formulated based on the requirements of the specific problem. When the decision variables of a problem are limited, the model is defined as a constrained model. [31]. When there are no constraints, the model is defined as an unconstrained model. Additionally, if the decision variables assume positive real values, it is referred to as continuous optimization; whereas, if all decision variables take integer values, it is termed a discrete optimization problem. Moreover, when only the immediate relationship is considered in the optimization problem, a static model is employed, whereas a dynamic model is used to portray the time-dependent changes in the system state. In addition to these distinctions, two types of optimization problems—single and multi-objective—can be considered to attain the desired design in the optimization process. [27,31,32].

## 5.1. Single Objective Optimization

In mathematically formulated design problems, the search for parameters that the model deems most suitable for a single design is known as single-objective optimization. It is important to note that subjective evaluations should be excluded unless clearly marked as such. Single-objective optimization refers to problems that feature a single objective function. This approach includes design variables, objective functions, constraints, and boundary constraints.[30,33]

The general mathematical definition of a single objective optimization problem is;

Minimize f (x)

where, $x = (x_1, x_2, x_3, \ldots, x_n)^T$

Subject to, $g_i(x) \leq 0 \qquad i = 1,2,\ldots,m$

$h_j(x) = 0 \qquad j = 1,2,\ldots,k$

In this case, the objective function (f(x)) represents the parameter that needs to be optimized while the design variable (x) refers to the parameters that determine the physical and functional characteristics of the system being designed. The assigned values for these parameters are known as limits (gi (x) and hj (x)). The optimization problem described above is typically formulated as a minimization problem. However is possible to change the sign of the objective function effectively converting the minimization problem into a maximization problem. As illustrated in Figure 18 maximizing -f(x) is equivalent to minimizing f(x).[30,33].

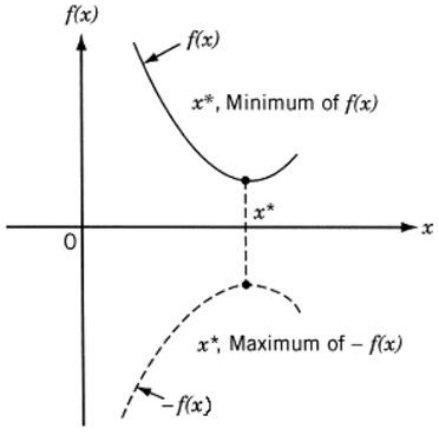


Figure 18. The minimum and maximum of the objective function f (x)

Technical problems encountered in everyday life often serve various purposes. Single-objective optimization algorithms may fail to yield meaningful results in the presence of conflicts, complexity, or when dealing with large objectives. As a result, the development of multi-objective optimization algorithms became necessary, aiming to address these challenges.

## 5.2. Multi Objective Optimization

Multi-objective optimization refers to the optimization of multiple objectives simultaneously. Many engineering problems in our daily lives require the optimization of conflicting objectives. For instance, a good spring design should be both lightweight and highly stiff. Similarly good vehicle design involves optimizing weight fuel economy and payload. It is crucial to recognize that a single solution may not exist that fulfills all the criteria in multi-objective optimization. Consequently, these problems can be converted into single-objective problems by assigning fixed weights to linear functions. However, prior to initiating the optimization process, determining the weights of the objective functions is essential, taking into account their respective significance. Additionally using single-objective optimization algorithms may not adequately explore the solution space and may not yield satisfactory results. In multi-objective optimization, objective functions can be optimized simultaneously. However, the challenge lies in finding the best point when not all objective functions reach their optimal values at the same point. The concept of scalar best commonly used in single-objective optimization cannot be applied in multi-objective optimization. Nevertheless, there are various methods for solving multi-objective problems with the Pareto optimal method being the most effective. Pareto analysis involves comparing vectors of objectives and their resulting solutions to determine dominance. This analysis helps to diversify the solution set ensuring a balance between the specified objectives. Therefore finding the Pareto optimal set is crucial in solving multi-objective optimization problems. [34,35].

The general mathematical definition of a multi-objective optimization problem can be expressed as follows:

Minimize $f_1(x), f_2(x), \ldots, f_r(x)$

where $x = (x_1, x_2, x_3, \ldots, x_n)^T$

Subject to,

$g_i(x) \leq 0 \qquad i = 1,2,\ldots,m$

$h_j(x) = 0 \qquad j = 1,2,\ldots,k$

In this context, the parameter intended for optimization is referred to as the objective function, while the parameters that specify the physical and functional attributes of the system to be designed are called design variables. The intervals within which the parameters can assume values are predefined and referred to as constraints.The optimization problem described above can be formulated as either a minimization or maximization problem [33].

## 5.3. Traditional and Non-Traditional Optimization Methods

Various optimization algorithms can be used to solve technical problems. These algorithms can be classified into two groups: traditional (deterministic) and non-traditional (stochastic) optimization methods.It is important to analyze the problem before selecting the appropriate method. Method of analysis, Lagrange coefficients, finite variation, etc. are traditional optimization methods and are only used for continuous and differentiable function problems. In the past, deterministic methods were employed to address technical challenges. However, in recent years, with the advancements in information technology, stochastic methods have gained prominence, particularly in domains traditionally dominated by deterministic approaches. Current stochastic methods, drawing inspiration from natural concepts and replicating them in a computerized environment, find applications in diverse fields. Their attributes, such as generating discrete solutions and achieving results close to the global optimum without requiring a predefined starting point, contribute to their widespread utilization. [27].

Genetic Algorithm(GA), Simulated Calcification(SA), Random Search(RS), Differential Evolution(DE), Particle Swarm Optimization(PSO), Ant Colony Optimization(ACO), Taboo Search(TS), Artificial Bee Colony(ABC), Markov Chain Monte Carlo(MCMC), Harmony Search(HS), Covariance Matrix Adaptation(CMA), Grenade Explosion Method(GEM) are stochastic optimization methods. In recent times, researchers have been actively refining these algorithms and introducing more efficient methods into the literature. Since the design and optimization problems of torsion

springs studied in this work have complex and non-linear functions, it was recommended to use stochastic optimization methods. In this context, the following subsections are detailed: Differential Evolution(DE), Simulated Annealing(SA), Random Search(RS), and Nelder-Mead(NM) algorithms, which are the preferred stochastic optimization methods in the study [27,33]. Two different optimization methods , Differential Evolution(MDE) and Nelder-Mead(MNM) were preferred for this thesis.

### 5.3.1. Nelder-Mead Algorithm

The classical Nelder-Mead (NM) derivative optimization technique, commonly known as the simplex search, was developed by John Nelder, Roger Mead, and Spendley in 1965. This method has found applications in various fields, including physics, chemistry, medicine, and engineering. Functioning as a traditional local search method, the Nelder-Mead algorithm is employed to locate the local minimum point in multidimensional unconstrained optimization problems. In addition, a simple is a polyhedron whose vertex is (n+1) in the n-dimensional search space and which gradually reaches the optimal point through an iterative process, i.e., it is also known as the best point search algorithm of these, because it is not a global algorithm,[36,37] it is not suitable for optimization problems with a large local minimum. However, with a small local sum, it can give good results for optimization problems. The Nelder-Mead algorithm yields favorable results in a shorter duration due to its ability to make substantial improvements in just a few iterations. As one of the non-linear and non-differentiable direct search algorithms, Nelder-Mead is an iterative method that involves four control parameters. These parameters consist of the reflection coefficient, expansion coefficient, contraction coefficient, and shrinkage factor. [38].

As constrained optimization problems are beyond the capability of conventional Nelder-Mead (NM), the algorithm can be adapted by incorporating a "penalty function" into the problem-solving algorithm. The initial step of the algorithm involves creating the first operational simplex (S). Subsequently, the minimization of the function directs the search path away from the vertex with the least favorable value in the function. This is achieved with a reflective and enhanced point. This improved algorithm uses a hybrid form with conjugate gradient and principal axis methods. A Nelder-Mead (MNM) algorithm was used in this thesis because the current optimization problems involve

nonlinear constraints and continuous design variables. [39] [40]. A flowchart of the algorithm is shown in Figure 19 [41].

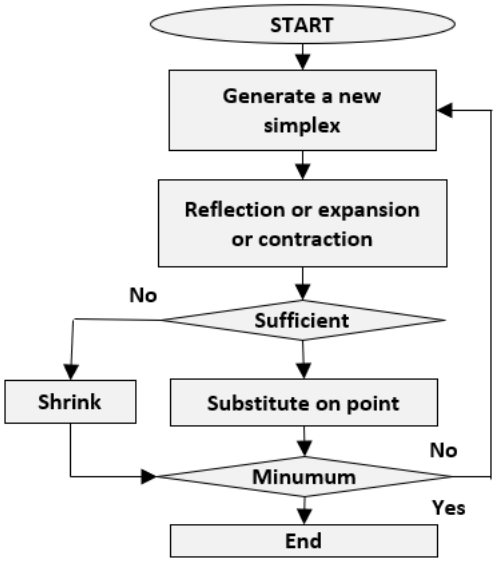


Figure 19. Nelder-Mead algorithm flowchart

## 5.3.2. Differential Evolution Algorithm

The differential evolution (DE) algorithm was introduced by Price and Storn in 1995 and is a multivariable metaheuristic algorithm. In addition, due to its operations and operators, it is a genetic algorithm-based population-based technique that provides significant results for continuous data optimization problems. DE, which is often used in continuous variable problems, is also used in discrete variables or combinations of continuous discrete variables Differential Evolution (DE) faces challenges when using an objective function instead of a fitness function and representing alternative solutions. DE does not operate with constraints; however, it is commonly employed to tackle problems integrated with an objective function of constraints. In comparison to other algorithms, DE stands out as one of the most efficient methods for real parameter optimization. The algorithm relies on three primary control parameters, namely differentiation/mutation constants, distribution constants, and population size, ensuring that each generation yields new populations with higher-quality individuals. Other control parameters of this algorithm are (i) the scale of the difficulty of the entire optimization case of the problem, (ii) the maximum number of generations called the

stopping condition, and (iii) the limit limit. The evolution process consisting of those parameters continues until the termination condition is met [42,43].

The Differential Evolution (MDE) algorithm is developed by making adjustments that can change the scaling factor and division frequency, which allows all solutions of the original DE algorithm to easily escape from stationarity. Thus, the algorithm's most apparent benefit is the scaling factor and transition speed of each solution.This thesis employed the MDE algorithm, and Figure 20 displays a flowchart of the algorithm.

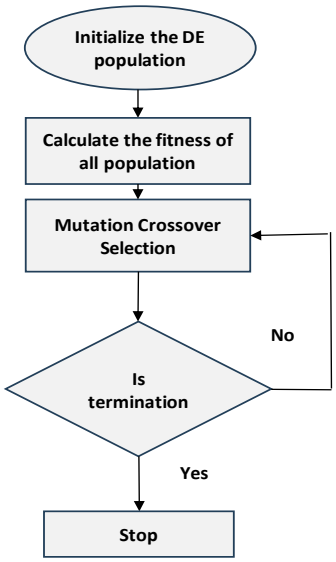


Figure 20. Flowchart of Differential Evolution Algorithm

# CHAPTER 6

## RESULTS AND DISCUSSION

This chapter analyses the results of the single lap joint test of the tested specimens. Subsequently, regression modelling and optimisation studies will be conducted.

## 6.1. Problem Statement

In this study, glass fiber reinforced polymer composites with different paste adhesive thicknesses, different paste adhesives and different peel plies were designed for the optimum shear strength on the bonding surfaces. Prior to obtaining the optimum design, first twelve different test samples were prepared regarding these three parameters, given in Table 2. Single lap joint tests were then performed on twelve different specimens in the MTS Landmark servo-hydraulic test system at the IZTECH laboratory in accordance with ASTM D5868-01. The obtained data for the strength values were used to obtain the suitable regression models. These models are the objective functions in optimization studies.

Table 2. Materials Description

| Inputs | Levels | Materials Name | Abridgment |
|---|---|---|---|
| **PEEL PLY** | 1 | Nylon | Nylon |
| | 2 | FLOGREEN | Green |
| | 3 | PA66 PA6 85R | PA |
| **ADHESIVE** | 1 | EPIKOTE Adhesive 1 | Adhs-1 |
| | 2 | EPIKOTE Adhesive 2 | Adhs-2 |
| **ADHESIVE THICKNESS** | 1 | 0.4 mm | 0.4 |
| | 2 | 0.6 mm | 0.6 |

## 6.2. Single Lap Joint Test Results

The composite plates were joined to two different paste adhesives. Test coupons are prepared according to ASTM D5868 standard. Figure 21. shows an image of a Single Lap Joints Test sample during testing. In the analysis, three types of peel ply and

two types of adhesives were used. Additionally, two types of adhesive thicknesses were used. Their names and abbreviations are shown in Table 2.

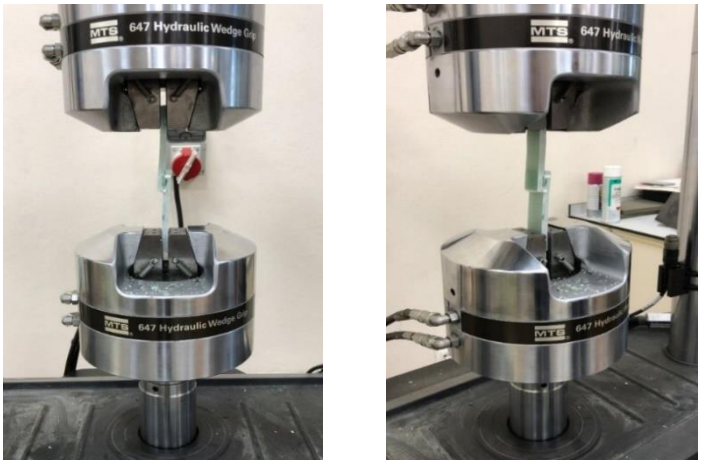


Figure 21. Single lap joints test

Firstly, performing the Single Lap Joint test, the samples were prepared according to ASTM D5868. The adhesion area of the samples prepared according to these standards has an area of 25mm*17mm. After the testing procedures were completed, the load applied to the sample piece on the device was divided by an area of 425 mm2 and the maximum stress value was calculated. The load-displacement figure is obtained with the single-lap joints test.

The average stress value of the sample with Adhs-1 adhesive, Nylon peel ply, and 0.4 mm thickness is 15.204 MPa. Load-displacement value of the "Adhs-1-Nylon-0.4" sample is shown in Figure 22. Five test samples were tested. Each one is shown in a different colour.

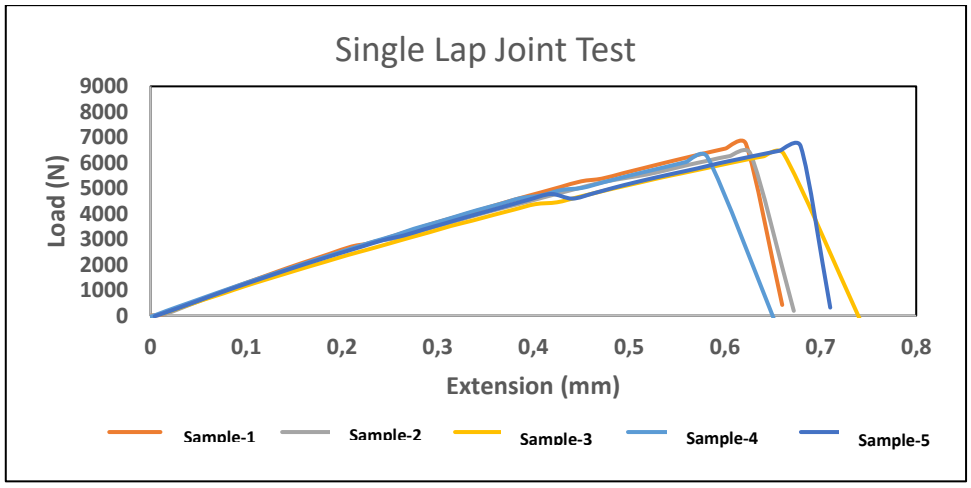


Figure 22. Single Lap Joint Test Load-Extension Diagram of Adsh-1-Nylon-0.4

The average stress value of the sample with Adhs-2 adhesive, Nylon peel ply, and 0.4 mm thickness is 7.434 MPa. Load-displacement value of the "Adhs-2-Nylon-0.4" sample is shown in Figure 23. Five test samples were tested. Each one is shown in a different colour.

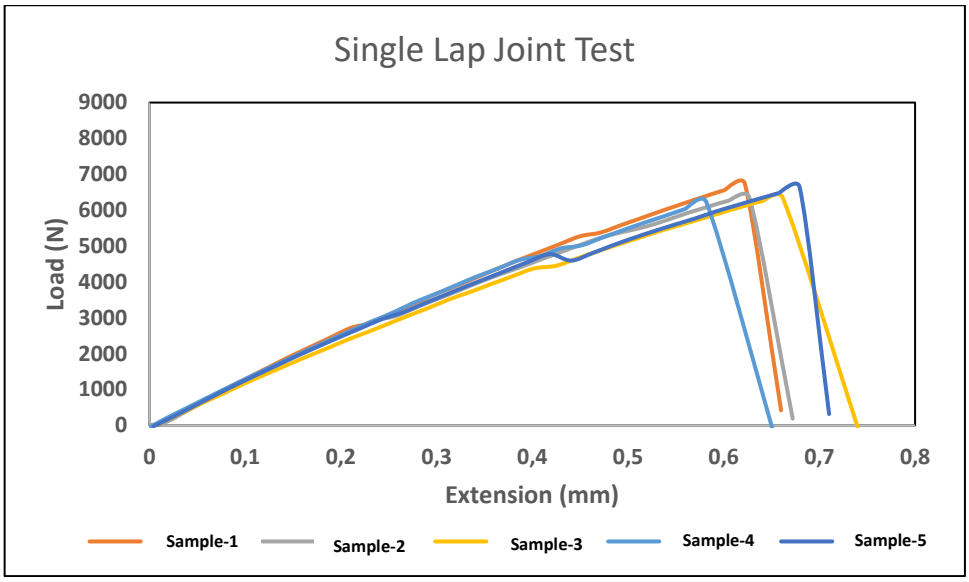


Figure 23. Single Lap Joint Test Load-Extension Diagram of Adsh-2-Nylon-0.4

The average stress value of the sample with Adhs-1 adhesive, Nylon peel ply, and 0.6 mm thickness is 17.110 MPa. Load-displacement value of the "Adhs-1-Nylon-0.6" sample is shown in Figure 24. Five test samples were tested. Each one is shown in a different colour.

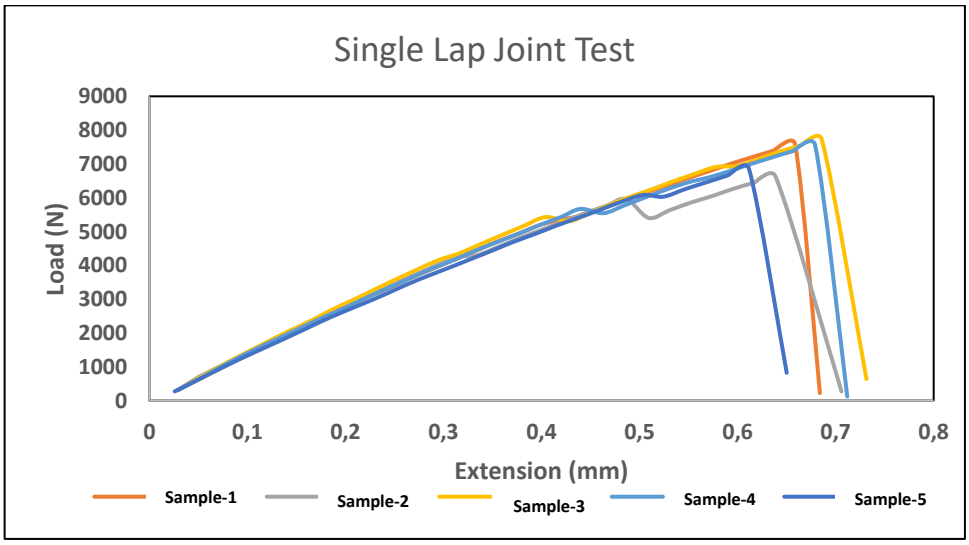


Figure 24. Single Lap Joint Test Load-Extension Diagram of Adsh-1-Nylon-0.6

The average stress value of the sample with Adhs-2 adhesive, Nylon peel ply, and 0.6 mm thickness is 7.853 MPa. Load-displacement value of the "Adhs-2-Nylon-0.6" sample is shown in Figure 25. Five test samples were tested. Each one is shown in a different colour.

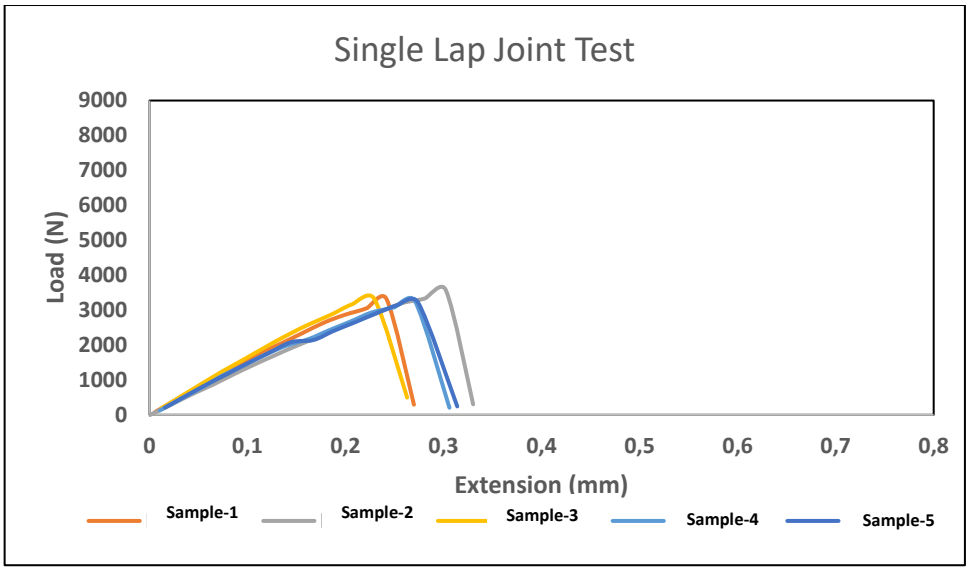


Figure 25. Single Lap Joint Test Load-Extension Diagram of Adsh-2-Nylon-0.6

The average stress value of the sample with Adhs-1 adhesive, PA peel ply, and 0.4 mm thickness is 15.651 MPa. Load-displacement value of the "Adhs-1-PA-0.4" sample is shown in Figure 26. Five test samples were tested. Each one is shown in a different colour.

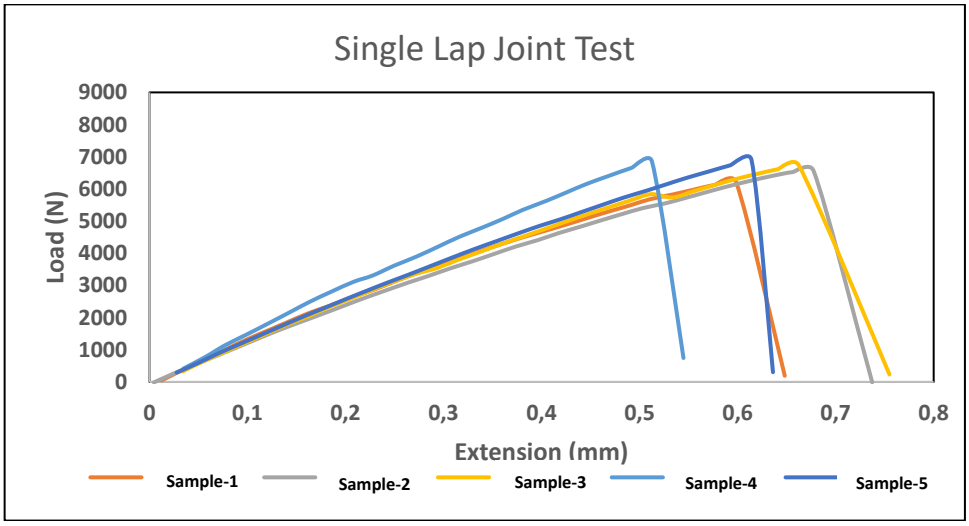


Figure 26. Single Lap Joint Test Load-Extension Diagram of Adsh-1-PA-0.4

The average stress value of the sample with Adhs-2 adhesive, PA peel ply, and 0.4 mm thickness is 6.699 MPa. Load-displacement value of the "Adhs-2-PA-0.4" sample is shown in Figure 27. Five test samples were tested. Each one is shown in a different colour.

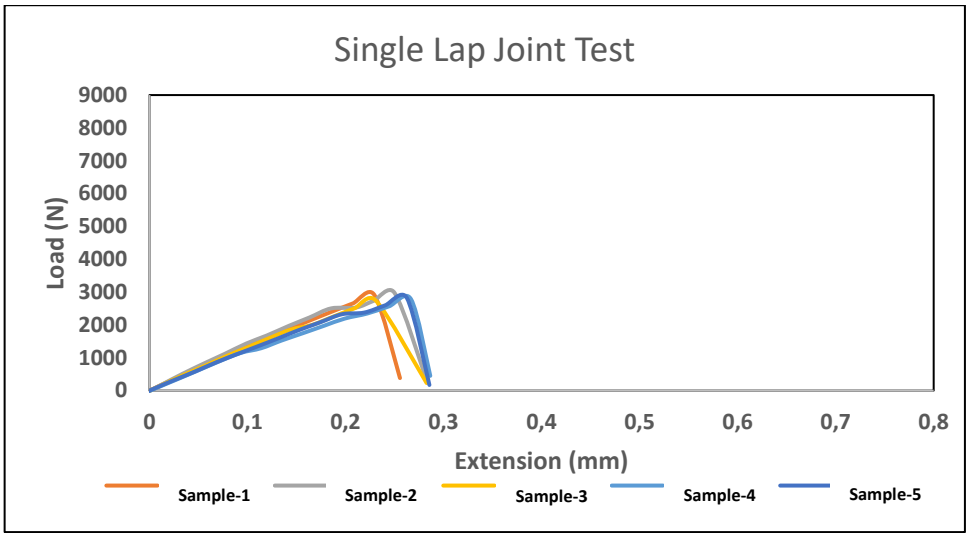


Figure 27. Single Lap Joint Test Load-Extension Diagram of Adsh-2-PA-0.4

The average stress value of the sample with Adhs-1 adhesive, PA peel ply, and 0.6 mm thickness is 16.938 MPa. Load-displacement value of the "Adhs-1-PA-0.6" sample is shown in Figure 28. Five test samples were tested. Each one is shown in a different colour.

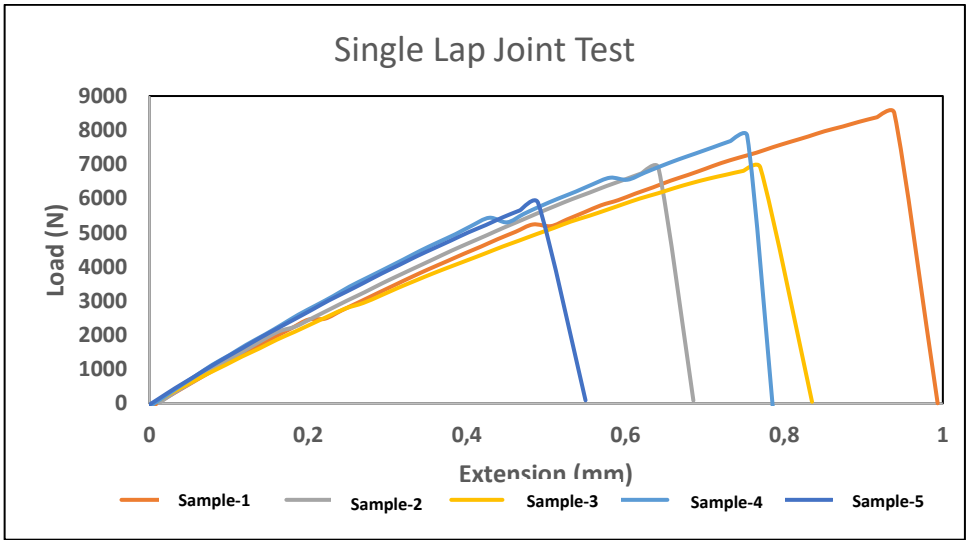


Figure 28. Single Lap Joint Test Load-Extension Diagram of Adsh-1-PA-0.6

The average stress value of the sample with Adhs-2 adhesive, PA peel ply, and 0.6 mm thickness is 8.992 MPa. Load-displacement value of the "Adhs-2-PA-0.6" sample is shown in Figure 29. Five test samples were tested. Each one is shown in a different colour.

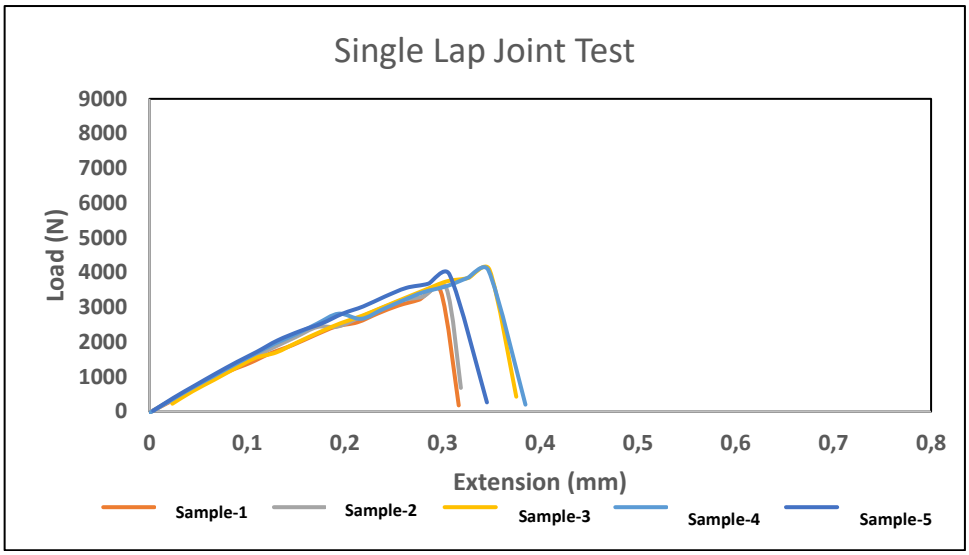


Figure 29. Single Lap Joint Test Load-Extension Diagram of Adsh-2-PA-0.6

The average stress value of the sample with Adhs-1 adhesive, Green peel ply, and 0.4 mm thickness is 14.648 MPa. Load-displacement value of the "Adhs-1-Green-0.4" sample is shown in Figure 30. Five test samples were tested. Each one is shown in a different colour.

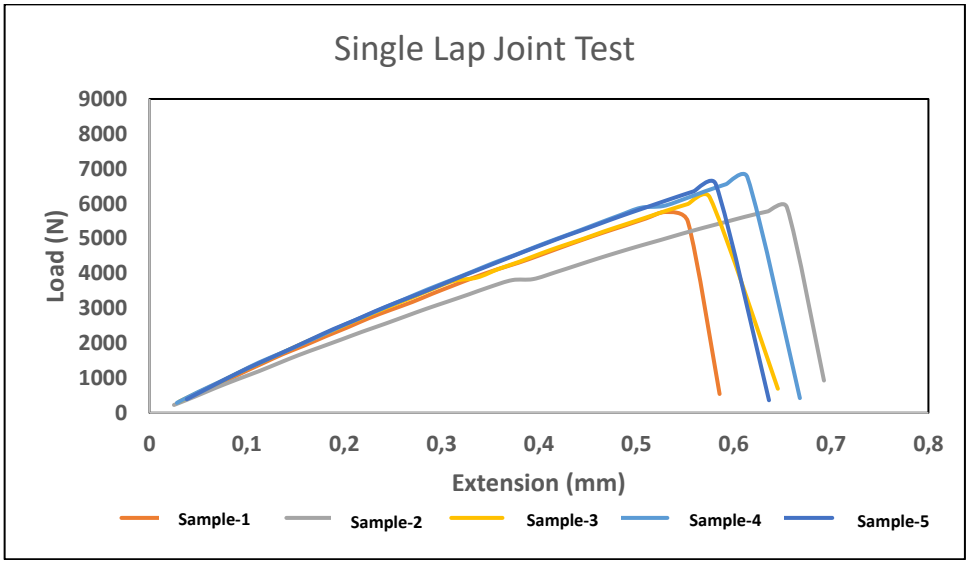


Figure 30. Single Lap Joint Test Load-Extension Diagram of Adsh-1-Green-0.4

The average stress value of the sample with Adhs-2 adhesive, Green peel ply, and 0.4 mm thickness is 7.606 MPa. Load-displacement value of the "Adhs-2-Green-0.4" sample is shown in Figure 31. Five test samples were tested. Each one is shown in a different colour.

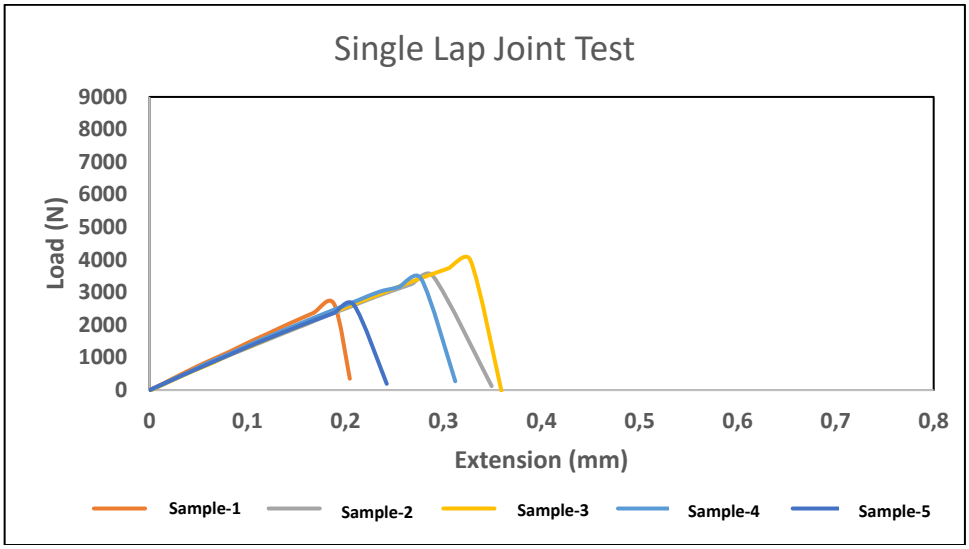


Figure 31. Single Lap Joint Test Load-Extension Diagram of Adsh-2-Green-0.4

The average stress value of the sample with Adhs-1 adhesive, Green peel ply, and 0.6 mm thickness is 18.251 MPa. Load-displacement value of the "Adhs-1-Green-0.6" sample is shown in Figure 32. Five test samples were tested. Each one is shown in a different colour.

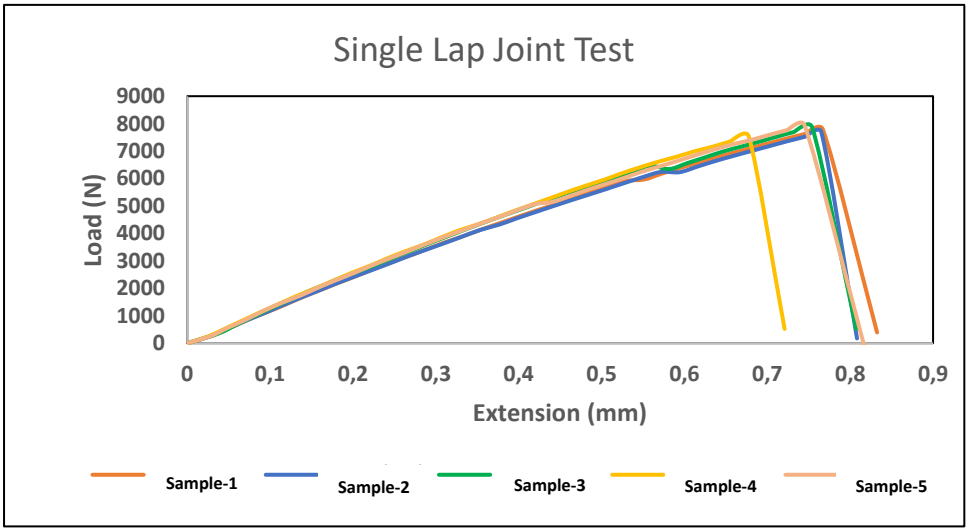


Figure 32. Single Lap Joint Test Load-Extension Diagram of Adsh-1-Green-0.6

The average stress value of the sample with Adhs-2 adhesive, Green peel ply, and 0.6 mm thickness is 10.617 MPa. Load-displacement value of the "Adhs-2-Green-0.6" sample is shown in Figure 33. Five test samples were tested. Each one is shown in a different colour.

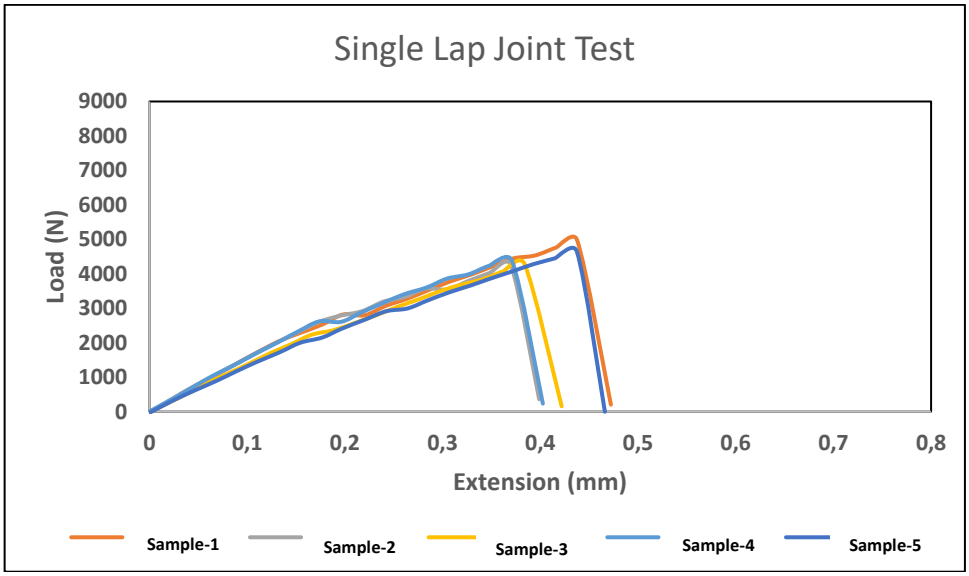


Figure 33. Single Lap Joint Test Load-Extension Diagram of Adsh-2-Green-0.6

Single Lap Joint testing of twelve different samples was performed. Five tests were performed on each sample. After these tests are carried out, the average shear stress values are given in Figure 34.

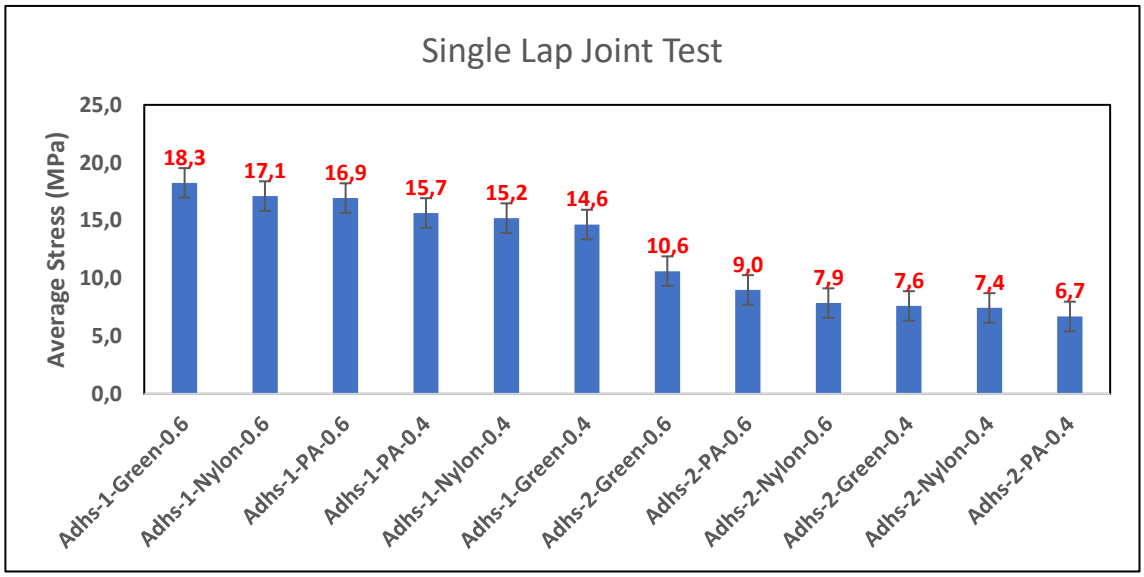


Figure 34. Single Lap Joints Test Results

By calculating the bonding area, stress values were calculated as shown in the figure above. In these Single Lap Joints tests, three different peel plies, two different paste adhesives, and two different adhesive thicknesses were examined, and the sample with the highest stress value and the effect of three different variables on the stress value were examined. Testing of 5 different samples from each different part was carried out. Critical differences were observed in the stress values of two different paste adhesives. The best bond strength was obtained in paste adhesive (EPIKOTE Adhesive 1) with a fast-curing temperature. In addition, it has been determined that the paste adhesive thickness has a serious effect on the bond strength. For example, if we compare the Adhs-1-Green-0.6 sample with the Adhs-1-Green-0.4 sample, the stress value of the Adhs-1-Green-0.6 sample is 18.3 MPa, while the stress value of the Adhs-1-Green-0.4 sample is 14.6 MPa. When other samples were compared according to their thickness, it was determined that the stress values of the samples with a thickness of 0.4 mm were lower than the stress values of the samples with a thickness of 0.6 mm.

When the samples with 0.6 mm paste adhesive thickness and EPIKOTE Adhesive 1 paste adhesive were examined, it was calculated that green peel ply had a higher stress value than other peel ply. However, when the samples with 0.4 mm paste adhesive thickness and EPIKOTE Adhesive 1 paste adhesive were examined, it was calculated that PA peel ply had a higher stress value than other peel ply. Looking at these results, when the stress values provided by three different peel plies were compared on the samples, it was determined that the peel plies did not create a major difference in the stress values of the parts.

The average stress value of the Adhs-1-Green-0.6 sample was obtained as the highest compared to the other samples. The average stress value of the Adhs-1-Green-0.6 sample was obtained as 18.3 MPa.

As can be seen from the Figure 35, in all tested samples cohesive failure mode is appeared.

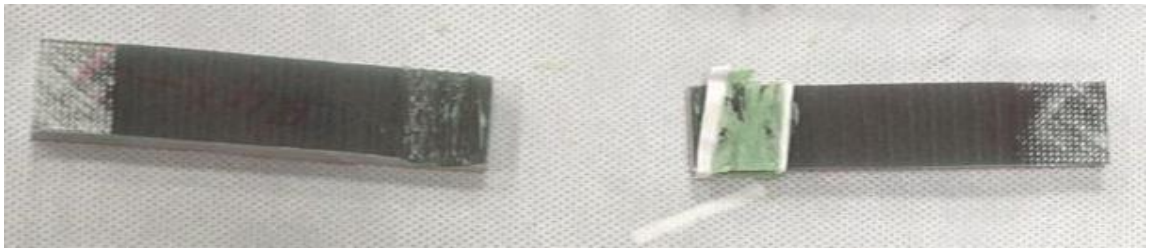

Figure 35. After test images of single lap joints test specimens

After the experimental studies were completed, regression models suitable for the problem addressed were created. Before creating regression models, experimentally performed single lap joint test results for twelve different samples are shown in Table3.

Table 3. The Average Shear Stress (MPa) Results of Test Samples

| | SAMPLE NAME | Stress (MPa) | Standard Deviation | Adhesive | Peel Ply | Paste Adhesive Thickness |
|---|---|---|---|---|---|---|
| **1** | Adhs-1-Green-0.6 | 18.251 | 0.336 | Adhs-1 | Green | 0.6 |
| **2** | Adhs-1-Green-0.4 | 14.648 | 0.893 | Adhs-1 | Green | 0.4 |
| **3** | Adhs-2-Green-0.6 | 10.617 | 0.638 | Adhs-2 | Green | 0.6 |
| **4** | Adhs-2-Green-0.4 | 7.606 | 1.250 | Adhs-2 | Green | 0.4 |
| **5** | Adhs-1-Nylon-0.6 | 17.110 | 1.037 | Adhs-1 | Nylon | 0.6 |
| **6** | Adhs-1-Nylon-0.4 | 15.204 | 0.453 | Adhs-1 | Nylon | 0.4 |
| **7** | Adhs-2-Nylon-0.6 | 7.853 | 0.292 | Adhs-2 | Nylon | 0.6 |
| **8** | Adhs-2-Nylon-0.4 | 7.434 | 0.389 | Adhs-2 | Nylon | 0.4 |
| **9** | Adhs-1-PA-0.6 | 16.938 | 2.118 | Adhs-1 | PA | 0.6 |
| **10** | Adhs-1-PA-0.4 | 15.651 | 0.586 | Adhs-1 | PA | 0.4 |
| **11** | Adhs-2-PA-0.6 | 8.992 | 0.613 | Adhs-2 | PA | 0.6 |
| **12** | Adhs-2-PA-0.4 | 6.699 | 0.195 | Adhs-2 | PA | 0.4 |

## 6.3. Regression Modeling Results

The stress optimization process in this thesis begins with mathematical modeling. At this stage, prior to the optimization process, the accuracy, robustness, and reliability of the optimization are increased by using regression analysis, which combines the strengths of traditional regression analysis. The functions obtained on the basis of regression models are given in Table 4. Related variables (inputs) in the table are as follows:

x1 : Adhesive, x2 : Peel Ply, x3 : Adhesive Thickness.

and the regression models' names are abbreviated as follows:

$P_1$ : Multiple linear,

$P_{1\text{-}R}$ : Multiple linear rational,

$P_2$ : Second order multiple non-linear,

$P_3$ : Third order multiple non-linear,

$P_4$ : Fourth order multiple non-linear,

$P_{2\text{-}R}$ : Second order multiple non-linear rational

Table 4. Mathematical functions obtained from regression analysis

| # | Type of Function | Obtained Functions fitted for Data set |
|---|---|---|
| 1 | $P_1$ | $-5.286 + 8.10017\,x1 + 0.084875\,x2 + 10.4325\,x3$ |
| 2 | $P_{1\text{-}R}$ | $\frac{-415.99 + 660.17x1 - 5.64x2 - 391.27x3}{-4.63 + 37.97x1 - 0.66x2 - 53.67x3}$ |
| 3 | $P_2$ | $-0.58 + 1.88x1 + 1.79x1^2 + 2.53x2 - 0.03x1x2 - 0.79x2^2 + 0.65x3 + 1.79x1x3 + 1.57x2x3 + 3.96x3^2$ |
| 4 | $P_3$ | $3.388 + 1.69x1 + 0.69x1^2 + 0.29x1^3 - 1.35x2 - 0.67x1x2 - 0.27x1^2x2 + 0.007x2^2 + 1.14x1x2^2 + 0.34x2^3 - 0.46x3 + 2.74x1x3 + 2.53x1^2x3 + 9.97x2x3 - 6.23x1x2x3 - 9.15x2^2x3 - 12.02x3^2 + 3.94x1x3^2 + 37.56x2x3^2 - 35.62x3^3$ |
| 5 | **$P_4$** | $2.95 + 1.47x1 + 0.61x1^2 + 0.25x1^3 + 0.11x1^4 - 0.28x2 - 0.36x1x2 - 0.25x1^2x2 - 0.14x1^3x2 - 0.16x2^2 + 0.16x1x2^2 + 0.17x1^2x2^2 + 0.02x2^3 + 0.22x1x2^3 + 0.03x2^4 + 2.04x3 + 1.49x1x3 + 0.83x1^2x3 + 0.43x1^3x3 + 2.403x2x3 + 0.193x1x2x3 - 0.393x1^2x2x3 - 0.5x2^2x3 - 1.76x1x2^2x3 - 0.79x2^3x3 - 2.29x3^2 + 0.44x1x3^2 + 0.924x1^2x3^2 + 8.894x2x3^2 + 1.78x1x2x3^2 - 1.27x2^2x3^2 - 12.01x3^3 - 2.33x1x3^3 + 21.31x2x3^3 - 30.05x3^4$ |
| 6 | **$P_{2\text{-}R}$** | $\frac{(42.91 + 52.12x1 + 70.53x1^2 + 16.28x2 - 94.15x1x2 + 9.05x2^2 + 9.33x3 - 9.013x1x3 - 79.55x2x3 - 0.73x3^2)}{(15.29 + 9.91x1 - 0.85x1^2 - 12.59x2 - 0.44x1x2 + 0.56x2^2 - 4.36x3 - 1.15x1x3 + 0.77x2x3 - 7.79x3^2)}$ |

At this stage of the thesis study, we aimed to use six different regression models from the existing literature. As a result, the optimization process involved creating mathematical models to estimate stress parameters and determine optimal values for process parameters according to desired specifications.

Table 5. Fit and boundedness check of the regression models

| # | Regression Model | $R^2$ Training | $R^2$ Training Adjusted | Maximum, Shear Strength, MPa | Minimum, Shear Strength, MPa |
|---|---|---|---|---|---|
| 1 | $P_1$ | 0.97 | 0.96 | 17.43 | 7.07 |
| 2 | $P_{1\text{-}R}$ | 0.99 | 0.98 | 10010 | -1342.85 |
| 3 | $P_2$ | 0.98 | 0.97 | 17.96 | 7.89 |
| 4 | $P_3$ | 0.99 | 0.99 | 18.19 | 6.72 |
| 5 | **$P_4$** | 1 | 1 | 18.25 | 6.69 |
| 6 | **$P_{2\text{-}R}$** | 1 | 1 | 18.25 | 6.69 |

Regression analysis and optimization studies are used to obtain more stable and optimum results. Therefore, among the regression models specified in Table 5. , $P_4$ and

$P_{2\text{-}R}$ regression models have been determined as the best regression models that accurately express the physical model and optimization studies will be carried out with them in section 6.3.2. $P_{1\text{-}R}$ model could also be chosen, but as the $R^2$ value went to 1, the min value was -1342.85 and the max value was 10010 MPa. That's why we didn't choose this.

## 6.4. Optimization Results

Optimization studies are used to obtain more stable and optimum results. The optimization procedure is set in MATHEMATICA according to the following definitions.

Find: $\{x_n, n\}$, where n is the number of variables, n=3,

x is the related variables (Adhesive, Peel Ply, Adhesive Thickness)

Maximum Iterations are 1000,

Firstly, if we were to define our problem, it is to find the maximum strength and minimum possible strength values with the above-mentioned parameters using Differential Evolution and Nelder-Mead algorithms. Table 6 shows the optimum designs for the defined problems.

Table 6. Results of the optimization problems for shear stress

| No | Objective Function | Optimization Algorithms | Minimum Value (MPa) | Minimum Shear Stress for Suggested Design | Maximum Value (MPa) | Maximum Shear Stress for Suggested Design | Optimization Problem Scenerios |
|---|---|---|---|---|---|---|---|
| 1 | $P_4$ | Differential Evolution | 6.669 | Adhesive = 1<br>Peel Ply = 3<br>Adhesive Thickness = 0.4 | 18.251 | Adhesive = 2<br>Peel Ply = 2<br>Adhesive Thickness = 0.6 | 1≤Adhesive≤2,<br>1≤Peel Ply≤3,<br>0.4≤Adhesive Thickness≤0.6 |
| | | Nelder Mead | 6.669 | Adhesive = 1<br>Peel Ply = 3<br>Adhesive Thickness = 0.4 | 16.938 | Adhesive = 2<br>Peel Ply = 3<br>Adhesive Thickness = 0.6 | 1≤Adhesive≤2,<br>1≤Peel Ply≤3,<br>0.4≤Adhesive Thickness≤0.6 |
| 2 | $P_{2\text{-}R}$ | Differential Evolution | 6.669 | Adhesive = 1<br>Peel Ply = 3<br>Adhesive Thickness = 0.4 | 18.251 | Adhesive = 2<br>Peel Ply = 2<br>Adhesive Thickness = 0.6 | 1≤Adhesive≤2,<br>1≤Peel Ply≤3,<br>0.4≤Adhesive Thickness≤0.6 |
| | | Nelder Mead | 6.669 | Adhesive = 1<br>Peel Ply = 3<br>Adhesive Thickness = 0.4 | 16.938 | Adhesive = 2<br>Peel Ply = 3<br>Adhesive Thickness = 0.6 | 1≤Adhesive≤2,<br>1≤Peel Ply≤3,<br>0.4≤Adhesive Thickness≤0.6 |

When the results in Table 6 are compared, the minimum values of both objective functions in the DE and NM optimization algorithms were 6.669 MPa. However, the maximum values of the DE optimization algorithm are different from the NM optimization algorithm. While the value of the DE optimization algorithm is equal to 18.251 MPa, the value of the NM optimization algorithm is equal to 16.938 MPa. As can be seen from here, NM optimization has a lower ability to maximize our problem than DE optimization.

In this thesis, additionally, as an optimization problem it is targeted to design a composite having the maximum shear strength of 16MPa. Optimization process were carried out with DE and NM algorithms using the regression models as an objective function. Optimization results of the design are shown in Table 7.

Table 7. Results of the optimization problem (targeted stress value of 16 MPa)

| # | Objective Function | Optimization Algorithms | Target Value (MPa) | Optimum Design Variables |
|---|---|---|---|---|
| 1 | $P_4$ | Differential Evolution | **16** | Adhesive=2,<br>Peel Ply=3,<br>Adhesive Thickness=0.430952 |
| | | | | Adhesive=2,<br>Peel Ply=1,<br>Adhesive Thickness=0.50285 |
| | | Nelder Mead | | Adhesive=2,<br>Peel Ply=1,<br>Adhesive Thickness=0.50285 |
| 2 | $P_{2\text{-}R}$ | Differential Evolution | | Adhesive=2,<br>Peel Ply=3,<br>Adhesive Thickness=0.430952 |
| | | | | Adhesive=2,<br>Peel Ply=1,<br>Adhesive Thickness=0.50285 |
| | | Nelder Mead | | Adhesive=2,<br>Peel Ply=1,<br>Adhesive Thickness=0.50285 |

When the results in Table 7. are compared, in the "Differential Evolution" optimization algorithms, the predicted design variables are Adhesive=2, Peel Ply=3, Adhesive Thickness=0.430952 for both objective functions to provide the targeted value of 16 MPa, or if it is a different estimated design variable Adhesive=2, Peel Ply=1, Adhesive Thickness =0.50283.

Additionally, in the "Nelder Mead" optimization algorithms, the predicted design variable for both objective functions to provide the targeted value of 16.00 MPa is Adhesive=2, Peel Ply=1, Adhesive Thickness=0.50283.

While "Differential Evolution" optimization algorithms found two alternative design for the targeted objective function, "Nelder Mead" optimization algorithms could only find only one.

# CHAPTER 7

# CONCLUSION

Composite materials are preferred by many sectors of the industry due to advantages such as lightness, durability, and high corrosion resistance. In addition, metal fasteners used to join composite materials cause negative effects such as delamination and weight increase in the composite. In recent years, researchers have been conducting research to develop adhesive bonding instead of metal fasteners.

In this study, three different parameters (adhesive type, adhesive thickness, and different brands of peel plies) were experimentally examined, and a regression model was created to examine the bonding strength of glass fiber reinforced polymer composites. Two different brands of paste adhesive with different curing times were bonded with paste adhesive by applying two different thicknesses, 0.4 and 0.6 mm. Surface preparation is essential to ensure good bond strength in adhesive. Three different brands of peel ply were used for surface preparation. In addition, the effect of these three particular parameters on bonding strength was examined experimentally and a mathematical regression model was created.

Single lap joints tests were performed on the test coupons prepared to examine the joint strength. Surface preparation is of critical importance in bonding strength. The three different peel plies used in this study showed similar performance in bond strength. This reveals that peel plies create similar roughness in the junction area. The curing times of the paste adhesive used are different. Curing time is important to save production time. In this study, fast-curing adhesive showed the best bonding performance. The fast-curing adhesive saves production time and increases bonding performance. Another parameter is the adhesive thickness. Experimental results have shown that 0.6 mm adhesive thickness improves the bonding performance.

The experimental results indicate that fast adhesive has a higher stress value than slow adhesive, and thick adhesive has a higher stress value than thin adhesive. The impact of three different peel ply types on stress value was not observed. The subsequent processes will consider the cost implications of material use in addition to stress values. Regression modeling and optimization studies were performed using the input and output data set in addition to the experimental inputs.

The stress optimization process in this thesis begins with the development of mathematical models. During this phase prior to the optimization process, the accuracy, robustness, and reliability of the optimization are increased by using Regression analysis, which is a combination of the strengths of the optimization. Six different regression models taken from the literature were used, and the two best regression models that accurately expressed the physical model were selected and an optimization study was carried out.

In the first of the optimization problems, the maximum strength and minimum strength values possible with the existing parameters were found by using Differential Evolution(DE) and Nelder Mead(NM) algorithms. When different optimization algorithm results were compared, it has been observed that the Nelder Mead optimization has a lower ability to maximize the stength than the Differential Evolution optimization.

In the second of the optimization problems, it was aimed to design a composite having the maximum strength of 16 MPa using DE and NM algorithms. It was observed that DE optimization algorithm found two alternative optimum design, however NM finds only one.

# REFERENCES


(1) Genç, Ç. , Arıcı. A. A. “Yat İmalatında Kullanılan CTP Malzeme ve İmalat Yöntemleri . *Gemi ve Deniz Teknolojisi Dergisi* **2008**, *178*, 6.

(2) Sathishkumar, T. P.; Satheeshkumar, S.; Naveen, J. Glass Fiber-Reinforced Polymer Composites - A Review. *Journal of Reinforced Plastics and Composites*. SAGE Publications Ltd **2014**, pp 1258–1275. https://doi.org/10.1177/0731684414530790.

(3) Mangino, E. ,. “The Research Requirements of The Transport Sectors to Facilitate An Increased Usage of Composite Materials.” **2007**, *44*.

(4) Banea, M. D.; Da Silva, L. F. M. Adhesively Bonded Joints in Composite Materials: An Overview. *Proceedings of the Institution of Mechanical Engineers, Part L: Journal of Materials: Design and Applications*. January 1, **2009**, pp 1–18. https://doi.org/10.1243/14644207JMDA219.

(5) Budhe, S.; Banea, M. D.; de Barros, S.; da Silva, L. F. M. An Updated Review of Adhesively Bonded Joints in Composite Materials. *Int J Adhes Adhes* **2017**, *72*, 30–42. https://doi.org/10.1016/j.ijadhadh.2016.10.010.

(6) Vinson, J. R. Adhesive Bonding of Polymer Composites. *Polymer Engineering and Science* **1989**, *29* (19), 1325–1331. https://doi.org/doi.org/10.1002/pen.760291904.

(7) Bénard, Q.; Fois, M.; Grisel, M. Peel Ply Surface Treatment for Composite Assemblies: Chemistry and Morphology Effects. *Compos Part A Appl Sci Manuf* **2005**, *36* (11), 1562–1568. https://doi.org/10.1016/j.compositesa.2005.02.012.

(8) Cotter, J. L.; Mahoon, A. Development of New Surface Pretreatments, Based on Alkaline Hydrogen Peroxide Solutions, for Adhesive BonN_n.g of Ttt Um. **1982**, 47. https://doi.org/10.1016/0143-7496(82)90066-5.

(9) Wingfield, J. R. J. Treatment of Composite Surfaces for Adhesive Bonding. **1993**, 151-156. https://doi.org/https://doi.org/10.1016/0143-7496(93)90036-9.

(10) Rangaswamy, H.; Sogalad, I.; Basavarajappa, S.; Acharya, S.; Manjunath Patel, G. C. Experimental Analysis and Prediction of Strength of Adhesive-Bonded Single-Lap Composite Joints: Taguchi and Artificial Neural Network Approaches. *SN Appl Sci* **2020**, *2* (6). https://doi.org/10.1007/s42452-020-2851-8.

(11) Vand H. , M.; Abbaszadeh, H.; Shishesaz, M. Optimization of Adhesive Single-Lap Joints under Bending Moment. *Journal of Adhesion* **2022**, *98* (11), 1687–1712. https://doi.org/10.1080/00218464.2021.1932485.

(12) Mehmet Erdem İriş. Karbon/Epoksi Kompozit Malzemelerden Yapilan Uçak Yapilarinda Yapişma Bağlantilari Mehmet Erdem İriş Yüksek Lisans Tezi Makina Mühendisliği Ana Bilim Dali Gazi Üniversitesi Fen Bilimleri Enstitüsü Mart **2020**.

(13) Kadıoğlu, F. Mechanical Behaviour of Adhesively Single Lap Joint under Buckling Conditions. *Chinese Journal of Aeronautics* **2021**, *34* (2), 154–164. https://doi.org/10.1016/j.cja.2020.06.010.

(14) Zhou, W.; A. S.; C. M.; Z. R.; H. R.; P. Y.; F. D. Preparation and Thermodynamic Analysis of the Porous ZrO2/(ZrO2+Ni) Functionally Graded Bolted Joint. *Compos. Part B Eng.* **2015**, *82* (1), 13–22. https://doi.org/doi.org/10.1016/j.compositesb.2015.07.018.

(15) Jones, R. M. *Design of Composite Structures*; **2015**. 46–155.

(16) Da Silva, L. F.; C. R. J. C.; C. G. W.; F. M. A. V.; B. K. Effect of Material, Geometry, Surface Treatment and Environment on the Shear Strength of Single Lap Joints. . *Int. J. Adhes. Adhes.* **2009**, *29* (6), 621–632. https://doi.org/doi.org/10.1016/j.ijadhadh.2009.02.012.

(17) Cognard, J. Y.; C. R.; M. J. Numerical Analysis of the Stress Distribution in Single-Lap Shear Tests under Elastic Assumption Application to the Optimisation of the Mechanical Behaviour. *Int J Adhes Adhes* **2011**, *31* (7), 715–724. https://doi.org/doi.org/10.1016/j.ijadhadh.2011.07.001.

(18) Lesh, R.; Harel, G. Problem Solving, Modeling, and Local Conceptual Development. *Math Think Learn* **2003**, *5* (2), 157–189. https://doi.org/10.1207/s15327833mtl0502&3_03.

(19) Sriraman B. , Are Giftedness and Creativity Synonyms in Mathematics? *The Journal of Secondary Gifted Education* **2005**, 20–36.

(20) Tutak T. , Y. G. Matematiksel Modellemenin Tanımı, Kapsamı ve Önemi. *Turkish Journal of Educational Studies* **2014**, 173–190.

(21) Küçükdoğan Ö. , N. Optimization of Delamination and Thrust Force in the Drilling Process of Nanocomposites. *European Journal of Science and Technology* **2021**, *32*, 807–815. https://doi.org/10.31590/ejosat.1040182.

(22) Pinder, J. P. ,. *Introduction to Business Analytics Using Simulation.* Academic Press: **2016**. 5–25.

(23) Erten H. İ. , Optimum Design and Analysis of Torsion Spring Used In Series Elastic Actuators for Rehabilitation Robots, Master's Thesis, Izmir Institute of Technology, **2022**.

(24) Devore, J. L. ,. *Probability and Statistics for Engineering and the Sciences*; Cengage Learning: **2015**. 468-593.

(25) Miles, J. R Squared, Adjusted R Squared. *Wiley StatsRef: Statistics Reference Online* **2005**. https://doi.org/doi.org/10.1002/9781118445112.stat06627.

(26) Sun, M.; Yang, J.; Cao, W.; Shao, J.; Wang, G.; Qu, H.; Huang, W.; Gong, X. Critical Process Parameter Identification of Manufacturing Processes of Astragali Radix Extract with a Weighted Determination Coefficient Method. *Chin Herb Med* **2020**, *12* (2), 125–132. https://doi.org/10.1016/j.chmed.2019.11.001.

(27) Erten, H. I.; D. H. A.; A. H. S. Designing Engineering Structures Using Stochastic Optimization Methods. **2020**. https://doi.org/https://doi.org/10.1201/9780429289576.

(28) Polatoğlu, İ.; A. L.; N. B. Ç.; Ö. S. ,. A Novel Approach for the Optimal Design of a Biosensor. *Anal Lett* **2020**, *57* (8), 1428–1445. https://doi.org/doi.org/10.1080/00032719.2019.1709075.

(29) Aydin, L.; Artem, H. S. Comparison of Stochastic Search Optimization Algorithms for the Laminated Composites under Mechanical and Hygrothermal Loadings. *Journal of Reinforced Plastics and Composites* **2011**, *30* (14), 1197–1212. https://doi.org/10.1177/0731684411415138.

(30) Xu, J.; Yang, P.; Liu, G.; Bai, Z.; Li, W. Constraint Handling in Constrained Optimization of a Storage Ring Multi-Bend-Achromat Lattice. *Nucl Instrum Methods Phys Res A* **2021**, *988*. https://doi.org/10.1016/j.nima.2020.164890.

(31) Yang, X.-S. ,. An Introduction with Metaheuristic Applications. *Engineering Optimization* **2010**, 271–272. https://doi.org/10.1002/9780470640425.

(32) Aydin, L.; A. O.; A. H. S.; M. A. ,. Design of Dimensionally Stable Composites Using Efficient Global Optimization Method. Proceedings of the Institution of Mechanical Engineers. *Design and Applications* **2016**, *233* (2). https://doi.org/doi.org/10.1177/1464420716664921.

(33) Venkata R. , V. J. S. Advanced Optimization Techniques. *Mechanical Design Optimization Using Advanced Optimization Techniques* **2012**, 5–34.

(34) Irisarri, F.-X.; B. D. H.; C. N.; M. J.-F. ,. Multiobjective Stacking Sequence Optimization for Laminated Composite Structures. *Composites Science and Technology* **2009**, *69* (7–8), 983–990. https://doi.org/doi.org/10.1016/j.compscitech.2009.01.011.

(35) Hasanoğlu, M. S.; Dölen, M. Comparison of Multi-Objective and Single-Objective Approaches in Feasibility Enhanced Particle Swarm Optimization. *Journal of the Faculty of Engineering and Architecture of Gazi University* **2020**, *35* (2), 887–900. https://doi.org/10.17341/gazimmfd.437579.

(36) Rajan, A.; Malakar, T. Optimal Reactive Power Dispatch Using Hybrid Nelder-Mead Simplex Based Firefly Algorithm. *International Journal of Electrical Power and Energy Systems* **2015**, *66*, 9–24. https://doi.org/10.1016/j.ijepes.2014.10.041.

(37) Nelder, J. A.; Meadf, R. A Simplex Method for Function Minimization. *Comput J* **1965**, *8* (1), 308–313. https://doi.org/doi.org/10.1093/comjnl/7.4.308.

(38) Xu, S.; Wang, Y.; Wang, Z. Parameter Estimation of Proton Exchange Membrane Fuel Cells Using Eagle Strategy Based on JAYA Algorithm and Nelder-Mead Simplex Method. *Energy* **2019**, *173*, 457–467. https://doi.org/10.1016/j.energy.2019.02.106.

(39) Ceylan, A. B. ; A. L. ; N. M. ; M. H. ; P. İ. ; S. H. ,. A New Hybrid Approach in Selection of Optimum Establishment Location of the Biogas Energy Production Plant. Biomass Conversion and Biorefinery. *Biomass Conversion and Biorefinery* **2021**, *13*, 5771–5786. https://doi.org/doi.org/10.1007/s13399-021-01532-8.

(40) Ozturk, S.; Aydin, L.; Celik, E. A Comprehensive Study on Slicing Processes Optimization of Silicon Ingot for Photovoltaic Applications. *Solar Energy* **2018**, *161*, 109–124. https://doi.org/10.1016/j.solener.2017.12.040.

(41) Barati, R. ,. Parameter Estimation of Nonlinear Muskingum Models Using Nelder-Mead Simplex Algorithm. *Journal of Hydrologic Engineering* **2011**, *16* (11). https://doi.org/doi.org/10.1061/(ASCE)HE.1943-5584.0000379.

(42) Das, S. ; S. P. N. ,. Differential Evolution: A Survey of the State-of-the-Art. IEEE Transactions on Evolutionary Computation. *IEEE* **2010**, 4–31. https://doi.org/10.1109/TEVC.2010.2059031.

(43) Storn, R. ; P. K. ,. Differential Evolution–A Simple and Efficient Heuristic for Global Optimization over Continuous Spaces. *Journal of global optimization* **1997**, *11*, 341–359. https://doi.org/doi.org/10.1023/A:1008202821328.